



## Model-observation and reanalyses comparison at key locations for heat transport to the Arctic

Assessment of key lower latitude influences on the Arctic and their simulation



Sunset over the North Atlantic Ocean. Credits: Ben Moat (NOC)

**Blue-Action: Arctic Impact on Weather and Climate** is a Research and Innovation action (RIA) funded by the Horizon 2020 Work programme topics addressed: BG-10-2016 Impact of Arctic changes on the weather and climate of the Northern Hemisphere. Start date: 1 December 2016. End date: 28 February 2021.



The Blue-Action project has received funding from the European Union's Horizon 2020 Research and Innovation Programme under Grant Agreement No 727852.

## Blue-Action Deliverable D2.1

### About this document

**Deliverable:** D2.1 Model-observation and reanalyses comparison at key locations for heat transport to the Arctic

**Work package in charge:** WP2 lower latitude drivers of arctic changes

**Actual delivery date for this deliverable:** 30 November 2019

**Dissemination level:** The general public (PU)

### Lead author

National Oceanography Centre (NOC): Ben I. Moat

### Other contributing authors

Centre National de la Recherche Scientifique (CNRS): Christophe Herbaut

Faroese Marine Research Institute (HAV): Karin Margetha Larsen, Bogi Hansen

National Oceanography Centre (NOC): Bablu Sinha, Ale Sanchez-Franks, Loic Houpert, Jenny Mecking, Simon Josey, Penny Holliday, Alejandra Sanchez-Franks

Netherlands eScience Center (NLeSC): Yang Liu, Jisk Attema, Wilco Hazeleger

National Center for Atmospheric Research (NCAR): Stephen Yeager, Justin Small

Marine and Freshwater Research Institute (MFRI): Hedinn Valdimarsson

Marine Scotland Science (MSS): Barbara Berx

Scottish Association for Marine Science (SAMS): Loic Houpert and Stuart Cunningham

University of Southampton (UoS): Samantha Hallam

University of Washington (UoW): Rebecca Woodgate, Craig Lee

Woods Hole Oceanographic Institution (WHOI): Young-Oh Kwon, Laura Flemming

### Contributing authors from non-partner organisations

Institut français de recherche pour l'exploitation de la mer (IFREMER): Herle Mercier

Bundesamts für Seeschifffahrt und Hydrographie (BSH): Kerstin Jochumsen

### Reviewer

National University of Ireland Maynooth (NUIM): Gerard McCarthy

### We support Blue Growth!

Visit us on: [www.blue-action.eu](http://www.blue-action.eu)



Follow us on Twitter: [@BG10Blueaction](https://twitter.com/BG10Blueaction)



Access our open access documents in Zenodo:

<https://www.zenodo.org/communities/blue-actionh2020>



Disclaimer: This material reflects only the author's view and the Commission is not responsible for any use that may be made of the information it contains.

|   |           |
|---|-----------|
| <b>Summary for publication</b>  | <b>5</b>  |
| <b>Work carried out</b>   | <b>6</b>  |
| <b>1.Comparison of observations of heat and freshwater transport to state-of-the-art coupled climate models</b>                                       | <b>6</b>  |
| <b>1.1 Introduction</b>   | <b>6</b>  |
| <b>1.2 Method</b>   | <b>8</b>  |
| <b>1.3 Evaluation of model transports at RAPID 26°N</b>   | <b>9</b>  |
| <b>1.4 Evaluation of model transports at the OVIDE section</b>  | <b>13</b> |
| <b>1.5 Evaluation of model transports at the OSNAP section</b>  | <b>14</b> |
| <b>1.6 Evaluation of model transports at the Greenland Scotland Ridge (GSR)</b>   | <b>18</b> |
| <b>1.7 Evaluation of model transports at the Davis Strait</b>   | <b>19</b> |
| <b>1.8 Evaluation of model transports at the Bering Strait</b>  | <b>21</b> |
| <b>1.9 Freshwater transports across the combined Davis Strait and GSR</b>   | <b>22</b> |
| <b>Partner contributions</b>  | <b>24</b> |
| <b>Non-partner Contributions</b>  | <b>24</b> |
| <b>2. Completion of in-situ ocean data (TMA dn GO-SHIP) with remote sensed data from Argo profiling floats, underwater gliders and satellite data</b> | <b>24</b> |
| <b>2.1 Argo Float profiles used at the RAPID 26°N Array</b>   | <b>24</b> |
| <b>2.2 Ocean glider and Altimetry at OSNAP</b>  | <b>25</b> |
| <b>2.3 Recreating the AMOC at 26°N using Altimetry</b>  | <b>27</b> |
| <b>2.4 Altimetry at the Greenland Scotland Ridge</b>  | <b>27</b> |
| <b>2.5 Altimetry at the GO-Ship A25 OVIDE section</b>   | <b>29</b> |
| <b>Partner Contributions</b>  | <b>30</b> |
| <b>Non-partner Contributions</b>  | <b>30</b> |
| <b>3. Examination of the correspondence between ocean heat transport estimates and atmospheric heat transport in the coupled model simulations</b>    | <b>30</b> |
| <b>3.1 Impact of Arctic climate change on North Atlantic Ocean circulation: a model study</b>   | <b>30</b> |
| <b>3.2 Atmospheric feedbacks in Coupled climate models.</b>   | <b>32</b> |
| <b>Partner contributions</b>  | <b>34</b> |
| <b>Main results achieved</b>  | <b>34</b> |
| <b>Progress beyond the state of the art</b>   | <b>41</b> |
| <b>Impact</b>   | <b>41</b> |

|  |           |
|--|-----------|
| <b>Lessons learned and Links built</b>                         | <b>42</b> |
| <b>Contribution to the top level objectives of Blue-Action</b> | <b>42</b> |
| <b>References (Bibliography)</b>                               | <b>44</b> |
| <b>Dissemination and exploitation of Blue-Action results</b>   | <b>46</b> |
| <b>Dissemination activities</b>                                | <b>46</b> |
| <b>Peer reviewed articles</b>                                  | <b>48</b> |
| <b>Other publications</b>                                      | <b>48</b> |
| <b>Uptake by the targeted audiences</b>                        | <b>49</b> |

## Summary for publication

Blue-Action Work Package 2 (WP2) focuses on lower latitude drivers of Arctic change, with a focus on the influence of the Atlantic Ocean and atmosphere on the Arctic. In particular, warm water travels from the Atlantic, across the Greenland-Scotland ridge, through the Norwegian Sea towards the Arctic. A large proportion of the heat transported northwards by the ocean is released to the atmosphere and carried eastward towards Europe by the prevailing westerly winds. This is an important contribution to northwestern Europe's mild climate. The remaining heat travels north into the Arctic. Variations in the amount of heat transported into the Arctic will influence the long term climate of the Northern Hemisphere. Here we assess how well the state of the art coupled climate models estimate this northwards transport of heat in the ocean, and how the atmospheric heat transport varies with changes in the ocean heat transport. We seek to improve the ocean monitoring systems that are in place by introducing measurements from ocean gliders, Argo floats and satellites.

These state of the art computer simulations are evaluated by comparison with key trans-Atlantic observations. In addition to the coupled models 'ocean-only' evaluations are made. In general the coupled model simulations have too much heat going into the Arctic region and the transports have too much variability. The models generally reproduce the variability of the Atlantic Meridional Ocean Circulation (AMOC) well. All models in this study have a too strong southwards transport of freshwater at 26°N in the North Atlantic, but the divergence between 26°N and Bering Straits is generally reproduced really well in all the models.

Altimetry from satellites have been used to reconstruct the ocean circulation 26°N in the Atlantic, over the Greenland Scotland Ridge and alongside ship based observations along the GO-SHIP OVIDE Section. Although it is still a challenge to estimate the ocean circulation at 26°N without using the RAPID 26°N array, satellites can be used to reconstruct the longer term ocean signal. The OSNAP project measures the oceanic transport of heat across a section which stretches from Canada to the UK, via Greenland. The project has used ocean gliders to great success to measure the transport on the eastern side of the array. Every 10 days up to 4000 Argo floats measure temperature and salinity in the top 2000m of the ocean, away from ocean boundaries, and report back the measurements via satellite. These data are employed at 26°N in the Atlantic to enable the calculation of the heat and freshwater transports.

As explained above, both ocean and atmosphere carry vast amounts of heat poleward in the Atlantic. In the long term average the Atlantic ocean releases large amounts of heat to the atmosphere between the subtropical and subpolar regions, heat which is then carried by the atmosphere to western Europe and the Arctic. On shorter timescales, interannual to decadal, the amounts of heat carried by ocean and atmosphere vary considerably. An important question is whether the total amount of heat transported, atmosphere plus ocean, remains roughly constant, whether significant amounts of heat are gained or lost from space and how the relative amount transported by the atmosphere and ocean change with time. This is an important distinction because the same amount of anomalous heat transport will have

## Blue-Action Deliverable D2.1

very different effects depending on whether it is transported by ocean or the atmosphere. For example the effects on Arctic sea ice will depend very much on whether the surface of the ice experiences anomalous warming by the atmosphere versus the base of the ice experiencing anomalous warming from the ocean. In Blue-Action we investigated the relationship between atmospheric and oceanic heat transports at key locations corresponding to the positions of observational arrays (RAPID at 26°N, OSNAP at ~55N, and the Denmark Strait, Iceland-Scotland Ridge and Davis Strait at ~67N) in a number of cutting edge high resolution coupled ocean-atmosphere simulations. We split the analysis into two different timescales, interannual to decadal (1-10 years) and multidecadal (greater than 10 years). In the 1-10 year case, the relationship between ocean and atmosphere transports is complex, but a robust result is that although there is little local correlation between oceanic and atmospheric heat transports, Correlations do occur at different latitudes. Thus increased oceanic heat transport at 26°N is accompanied by reduced heat transport at ~50N and a longitudinal shift in the location of atmospheric flow of heat into the Arctic. Conversely, on longer timescales, there appears to be a much stronger local compensation between oceanic and atmospheric heat transport i.e. Bjerknes compensation.

## Work carried out

Deliverable D2.1 is broadly linked to the following tasks in WP2:

- Assessment of key lower latitude influences on the Arctic and their simulation (Task 2.1)
- Pathways and interactions sustaining Arctic predictability (Task 2.2)
- Optimization and coordination of existing TMA systems, improved data delivery for predictions and identification of gaps (Task 2.3).

More in detail, the work presented in this deliverable directly contributes to the following activities:

- At key locations, Blue-Action compares observations of heat and freshwater transport to state-of-the-art coupled climate models (HadGEM-Charisma, IPSL, CESM) and high resolution ocean-only models e.g., NEMO (1/24°)
- In-situ ocean data originating from transport mooring arrays (TMAs) and hydrographic GO-SHIP sections are complemented with remote sensed data from Argo profiling floats, from underwater gliders and satellite data (including existing missions, and new missions data from Jason-3 and Sentinel-3, when they are operational).
- Correspondence, compensation or feedback between these ocean heat transport estimates and atmospheric heat transport are examined in the coupled model simulations.

## 1.Comparison of observations of heat and freshwater transport to state-of-the-art coupled climate models

### 1.1 Introduction

There is a northward transport of heat throughout the whole Atlantic Ocean, reaching a maximum of 1.3PW (25% of the global heat flux) around 24.5°N in the subtropical North Atlantic. The heat transport is a balance of the northward transport of a warm Gulf Stream, and a southward

## Blue-Action Deliverable D2.1

transport of thermocline and cold North Atlantic Deep Water that is known as the meridional overturning circulation (AMOC). The heat transported by the AMOC is given off to the atmosphere and much of it is carried eastward by the prevailing westerly winds. This is an important contribution to northwestern Europe's mild climate. The latest IPCC Special Report on Ocean and Cryosphere (IPCC, 2019) states that both in situ (2004–2017) and based on sea surface temperature reconstructions, indicate that the Atlantic Meridional Overturning Circulation (AMOC) has weakened relative to 1850–1900. CMIP5 model simulations of the period 1850–2015, on average, exhibit a weakening AMOC when driven by anthropogenic greenhouse gas forcing. Therefore it is critical that we evaluate the next generation of very high resolution models to better understand and predict our changing climate.

The latest state-of-the-art climate models are compared with observational estimates to evaluate their accuracy in predicting the magnitude and variability of North Atlantic heat and freshwater transports into the Arctic region. Observations of oceanic heat and freshwater transports have been compared with estimates from the following state-of-the-art coupled climate models: 1) a 100 year control run of the HadGEM-Charisma 1/12° ocean coupled to a N512 (25km) atmosphere, 2) a 53 year historical run of the HadGEM-Charisma 1/12° ocean coupled to a N512 (25km) atmosphere, 3) an 80 year control run of the Community Earth System Model 1/10° ocean coupled to ¼° atmosphere (Small et al. 2014). The control run of the HadGEM-Charisma model was run by the UK Met office as part of the H2020 project PRIMAVERA ( <https://www.primavera-h2020.eu/> ) and the historical run of the HadGEM-Charisma was run by NOC, UK as part of the ACSIS project ( <http://www.acsis.ac.uk/> ). An overview of the HadGEM-Charisma coupled models are available (Roberts et al., 2019). Included in the study was a 54 year run of a high resolution ocean only global model run at a 1/12° resolution (Moat et al., 2016; Madec., 2008). As part of the Blue Action project a ¼° degree ocean only global model with a North Atlantic 1/24° nest has been run for 10 years and evaluated here. The 1/24° nest was embedded between 28N and the Bering Strait. The HadGEM-Charisma, 1/12° high resolution ocean only global model and the 1/24° model are all based on the NEMO ORCA global ocean circulation model.

Significant delays have been experienced in running both the HadGEM-Charisma control and historical coupled models. A freshwater imbalance in both models was discovered after months of simulation, which then required the fault to be identified and each simulation rerun from the beginning. As it takes 3.5 days to run one year of model time, this rerun has taken considerable time. The control simulation completed the full 100 years in 2019, but the historical simulation has only been run for 60 years up to the publication of this report. Both the ocean transport evaluation and the atmospheric model feedback and compensation has been completed in 2019 and not yet been written into a paper. IPSL coupled model simulations required to analyse as part of D2.1 are not available ( See D2.6 report ).

Observations used in this evaluation include the RAPID AMOC mooring array at 26°N (Smeed, et al. 2019), OSNAP array (Lozier et al., 2019), OVIDE ship Section (Mercier et al, 2016), Greenland Scotland Ridge array (Østerhus et al., 2019), Bering Strait mooring array (Woodgate, 2018) and Davis Strait mooring array (Curry et al., 2014). There is currently no AMOC time series or heat transport at the Extended Ellett line and therefore no model observation evaluation is included in this report. The locations of these transport mooring arrays (TMA) and hydrographic Sections are shown in Figure 1.

In this section we will go through the method used to calculate the heat and freshwater transports (Section 1.2) and then show the comparisons between models and observations in turn (Sections 1.3 to 1.8). We will conclude our main results in Section 4.

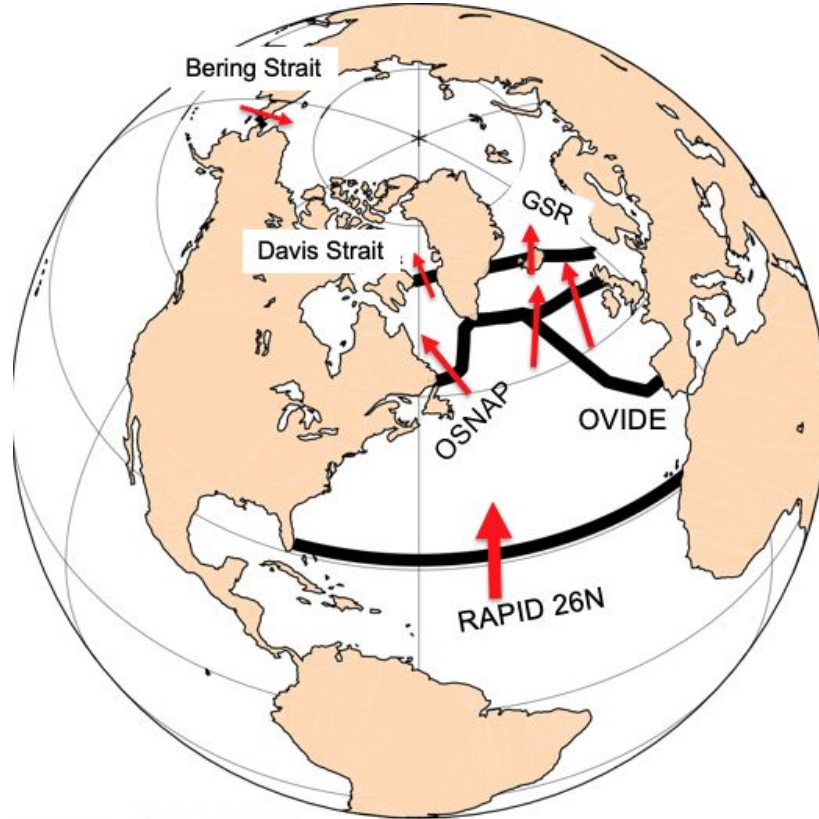


**Figure 1.** The locations of the North Atlantic observational Arrays and the hydrographic ship sections. The arrows indicate the direction of the oceanic heat transport towards the Arctic.

## 1.2 Method

The model estimates of the Atlantic Meridional Overturning Circulation (AMOC) is defined as the maximum of the overturning streamfunction. Across the RAPID 26°N section this is defined in z levels after the RAPID 26°N methodology (McCarthy et al , 2015). At the OSNAP and OVIDE sections this is defined in the same way as observations in density space, with density calculated relative to the surface at OSNAP ( $\sigma_0$ ) and 1000m at OVIDE ( $\sigma_1$ ). The AMOC and heat transports were not calculated at the Bering Straits, Davis Strait and Greenland Scotland Ridge sections. Instead volume, temperature transports were calculated to enable comparison with observation. The models use the meridional velocity field directly from the model rather than using a geostrophic estimate of the velocity. The velocity field used to estimate the AMOC has been adjusted to be zero net volume transport.

The meridional temperature transport (TT), heat transport (HT) and salinity transport (ST) are defined as:

$$TT = \rho C_p \iint v \theta \, dx dz \quad (1)$$

$$HT = \rho C_p \iint v_c \theta \, dx dz \quad (2)$$

## Blue-Action Deliverable D2.1

$$ST = \iint v_c S dx dz \quad (3)$$

were  $\rho C_p = 4.1 \times 10^6 \text{ J m}^{-3} \text{ kg}^{-1}$ ,  $v$  is the model meridional velocity,  $v_c$  is the model meridional velocity compensated to zero net volume transport across an ocean section,  $\theta$  is the potential temperature and  $S$  is the salinity.

The freshwater transport and its divergence from the Bering Straits inflow follow the methodology of McDonagh et al., (2015). The freshwater transport ( $F_W$ ) is defined as

$$F_W = \frac{1}{\bar{s}}(ST - ST_{BS}) \quad (4)$$

where  $\bar{s}$  is the average salinity of the section (e.g. the salinity across the 26N section),  $ST$  is the salinity transport across the section and  $ST_{BS}$  is the salinity transport through the Bering Straits. The divergence of the freshwater transport is the difference between  $F_W$  at each section and the freshwater transported through the Bering Straits. The freshwater transports and their divergence from the Bering Straits was calculated for the RAPID 26°N section, OSNAP, and the combined Davis Strait and Greenland-Scotland Ridge.

All oceanic transports are calculated from monthly model averages and filtered annually. The models will be referred to as; coupled climate control run (CONTROL), coupled climate historical run (HIST), Community Earth System Model High resolution run (CESM-H), NEMO 1/12° forced run (NEMO12), and NEMO 1/24° forced run (NEMO24). Due to model drift in CESM-H we will only be evaluating the last 20 years of the run (1960 to 1980).

### 1.3 Evaluation of model transports at RAPID 26°N

The RAPID AMOC programme has been monitoring the Atlantic Meridional Overturning Circulation (AMOC) at 26°N and the associated heat and freshwater transports continuously since 2004 (Smeed et al. 2018; Bryden et al, 2019). Model estimates of AMOC, heat transport, freshwater transport, and freshwater transport divergence from the Bering Straits are evaluated against observation in Figure 2 and detailed in Table 1. The observed average AMOC from monthly mean values between April 2004 and September 2018 is  $17.7 \pm 3.45 \text{ Sv}$  (Cyan, Fig. 2). The AMOC in the CONTROL and HIST model runs are higher than observation ( 21 Sv and 21 Sv, vs 18 Sv from observation) and result in a very good heat transport comparison with observation ( 1.3 PW and 1.2 PW, vs 1.2 PW from observation). The linear relationship between AMOC and heat transport holds at 26°N in the models (Figure 3). The AMOC in the CESMH model ( 18.5 Sv) has a reasonable agreement with observation ( 17.7 Sv ). The heat transport in CESMH is slightly low, but has possibly the closest relationship between AMOC and heat of the models included in this study (Figure 3). The NEMO12 hindcast has a lower than observation AMOC and heat transport ( 15.3 Sv ). The CONTROL and HIST models reproduce the variability of the AMOC well. All models in this study have a too strong southwards transport of freshwater at 26°N, but the divergence between 26°N and Bering Straits is reproduced well (within 0.1 Sv of observation) in all the models, except the NEMO12 which is slightly low (within 0.2 Sv observation).

## Blue-Action Deliverable D2.1

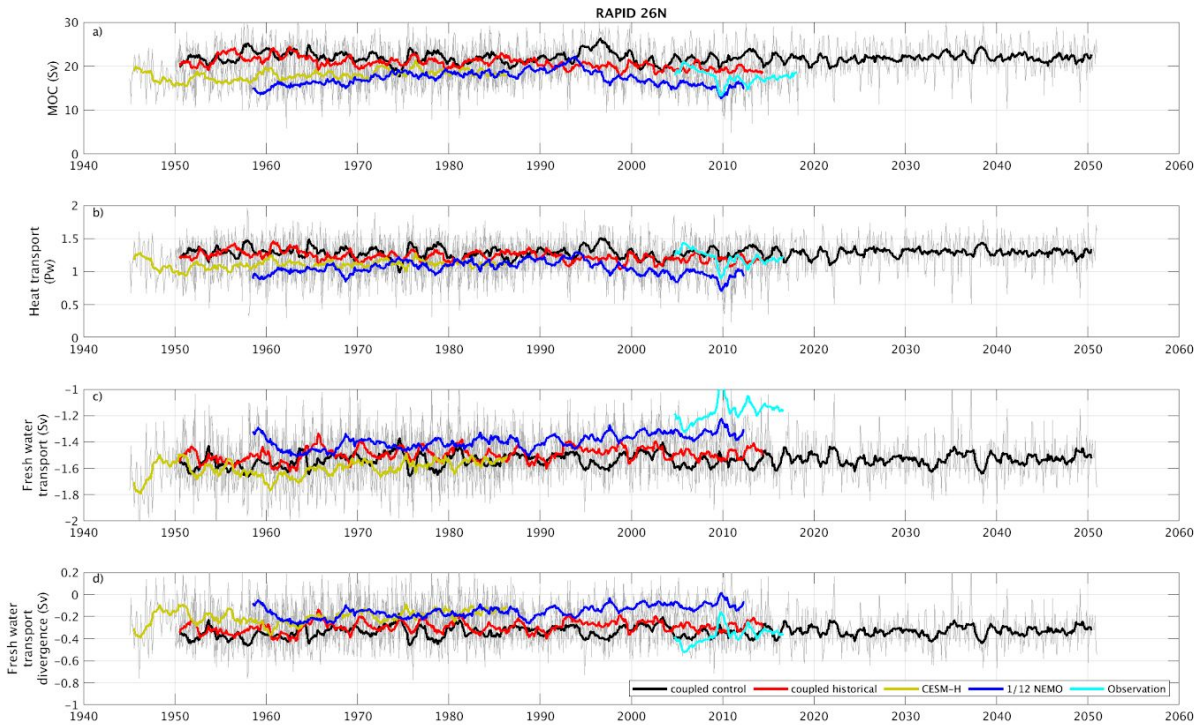


**Figure 2.** Comparison of observations and the various models at the RAPID 26°N section. AMOC (a), heat transport (b) and fresh water transport, and c) fresh water divergence from the Bering Straits.

There is a high degree of correlation between the heat transport and the AMOC through all the models ( $r^2 > 0.8$ ) and observations ( $r^2 = 0.9$ ). Figure 3 and Table 2 show the regression between heat transport and the AMOC for observation and models. For a given AMOC strength, the heat transport tends to be underestimated in all the models. However, the models do reproduce the slope of the relationship well (b-value in Table 2) suggesting that the vertical stratification in the models is well represented. The observed sensitivity of the heat transport to a change in the strength of the AMOC is 0.075 PW per Sverdrup of AMOC variation (Table 2). The models are typically around 0.06 PW per Sverdrup, with the CESMH around 0.07 PW per Sverdrup.

Blue-Action Deliverable D2.1

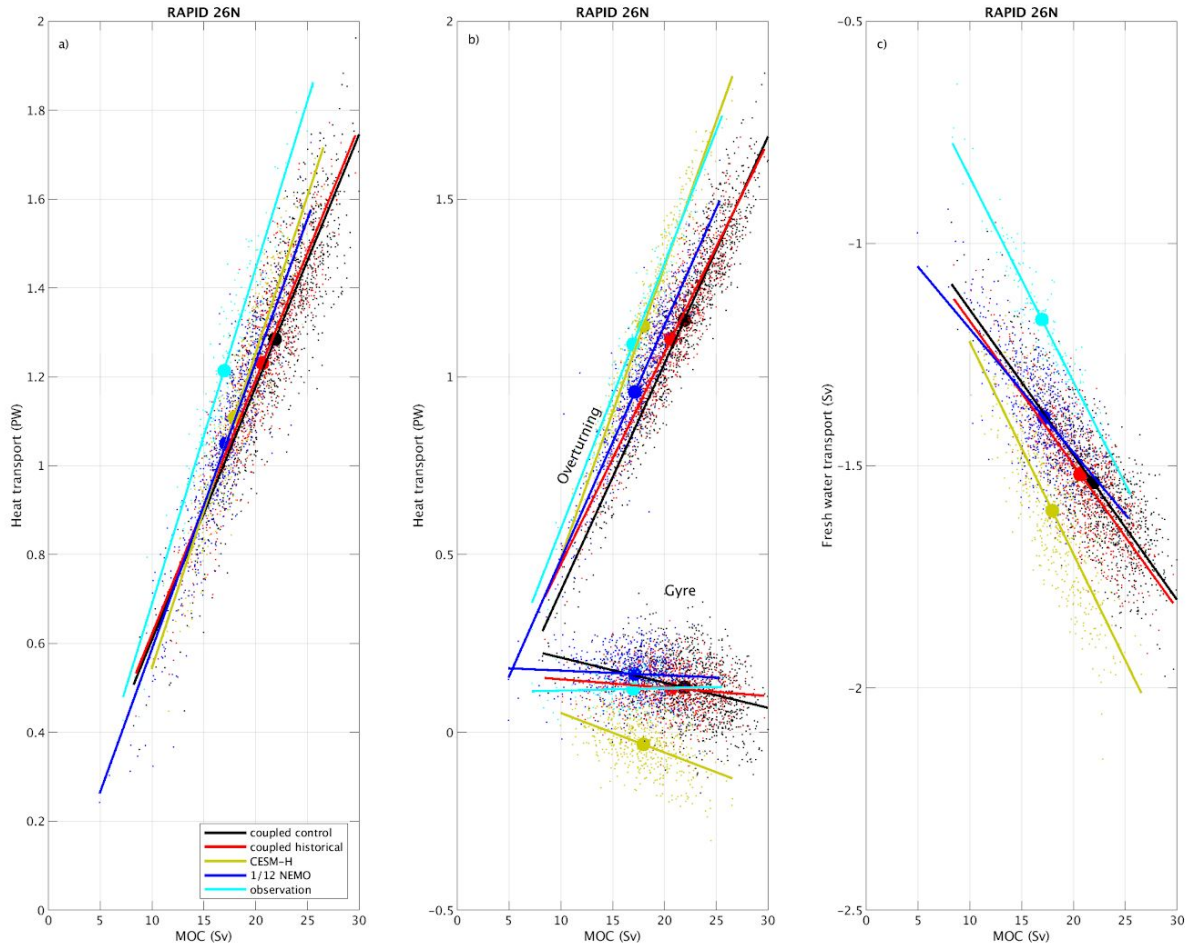


**Figure 3.** The relationship between the AMOC at 26°N and the a) heat transport, b) the components of the heat transport and c) fresh water transports across the RAPID 26°N section.

**Blue-Action Deliverable D2.1**

|  | AMOC<br>(Sv) | Heat transport<br>(PW) | Freshwater<br>Transport<br>(Sv) | Freshwater<br>Transport<br>divergence<br>(Sv) |
|--|--------------|------------------------|---------------------------------|---|
| HADGEM3<br>Control   | 21.90 ± 3.74 | 1.28 ± 0.24            | -1.54 ± 0.15                    | -0.34 ± 0.15                                  |
| HADGEM3<br>Historical  | 20.65 ± 3.39 | 1.23 ± 0.21            | -1.52 ± 0.14                    | -0.32 ± 0.14                                  |
| CESM-H   | 18.48 ± 2.91 | 1.12 ± 0.23            | -1.57 ± 0.17                    | -0.21 ± 0.11                                  |
| NEMO12   | 15.25 ± 2.91 | 0.93 ± 0.22            | -1.33 ± 0.11                    | -0.10 ± 0.11                                  |
| NEMO24   | n/a          | n/a                    | n/a                             | n/a   |
| Observation<br>( Smeed et al, 2019)<br>( McDonagh et al 2015)<br>(Johns et al. 2011) | 17.66 ± 3.45 | 1.21 ± 0.25            | -1.17 ± 0.16                    | -0.37 ± 0.16                                  |

**Table 1.** Mean AMOC, transports of heat and freshwater, and the freshwater divergence at the RAPID 26°N section. The means for the NEMO12 hindcast simulation are for the RAPID period only. There is no high resolution fields from the NEMO24 model at 26°N so it has not been included.

|  | Relationship between AMOC and<br>heat transport<br><br>HT = a+b*AMOC | Relationship between AMOC and fresh<br>water transport<br><br>FW = a+b*AMOC |
|--|--|---|
| HADGEM3 Control  | a= 0.039, b= 0.057, r <sup>2</sup> =0.80                             | a= -0.82, b= -0.033, r <sup>2</sup> =0.67                                   |
| HADGEM3<br>Historical  | a= 0.050, b= 0.057, r <sup>2</sup> =0.82                             | a= -0.85, b= -0.032, r <sup>2</sup> =0.66                                   |
| CESM-H   | a= -0.16, b= 0.071, r <sup>2</sup> =0.87                             | a= -0.75, b= -0.048, r <sup>2</sup> =0.67                                   |
| NEMO12   | a= -0.056, b= 0.064, r <sup>2</sup> =0.83                            | a= -0.91, b= -0.028, r <sup>2</sup> =0.51                                   |
| NEMO24   | n/a  | n/a   |
| Observation<br>( Smeed et al, 2019)<br>( McDonagh et al 2015)<br>(Johns et al. 2011) | a= -0.064, b= 0.075, r <sup>2</sup> =0.92                            | a= -0.39, b= -0.046, r <sup>2</sup> =0.90                                   |

**Table 2.** Linear regression coefficients from Figure 3 a) and c). There is no high resolution fields from the NEMO24 model at 26°N so it has not been included.

**1.4 Evaluation of model transports at the OVIDE section**

An observational monthly time series of the upper limb of the Atlantic meridional overturning circulation (AMOC) intensity at the GO-SHIP A25 Greenland-Portugal OVIDE line from 1993 to 2017 is available (Mercier et al., 2015, <https://www.seanoe.org/data/00353/46445/>). The AMOC time series was derived by combining AVISO altimetry with ISAS temperature and salinity data (Figure 4, Contributes to Task 2 of D2.1 and is covered in Section 2.5). In addition, ship based estimates of the AMOC and Heat transport are produced every 2 years (symbols in Figure 4).

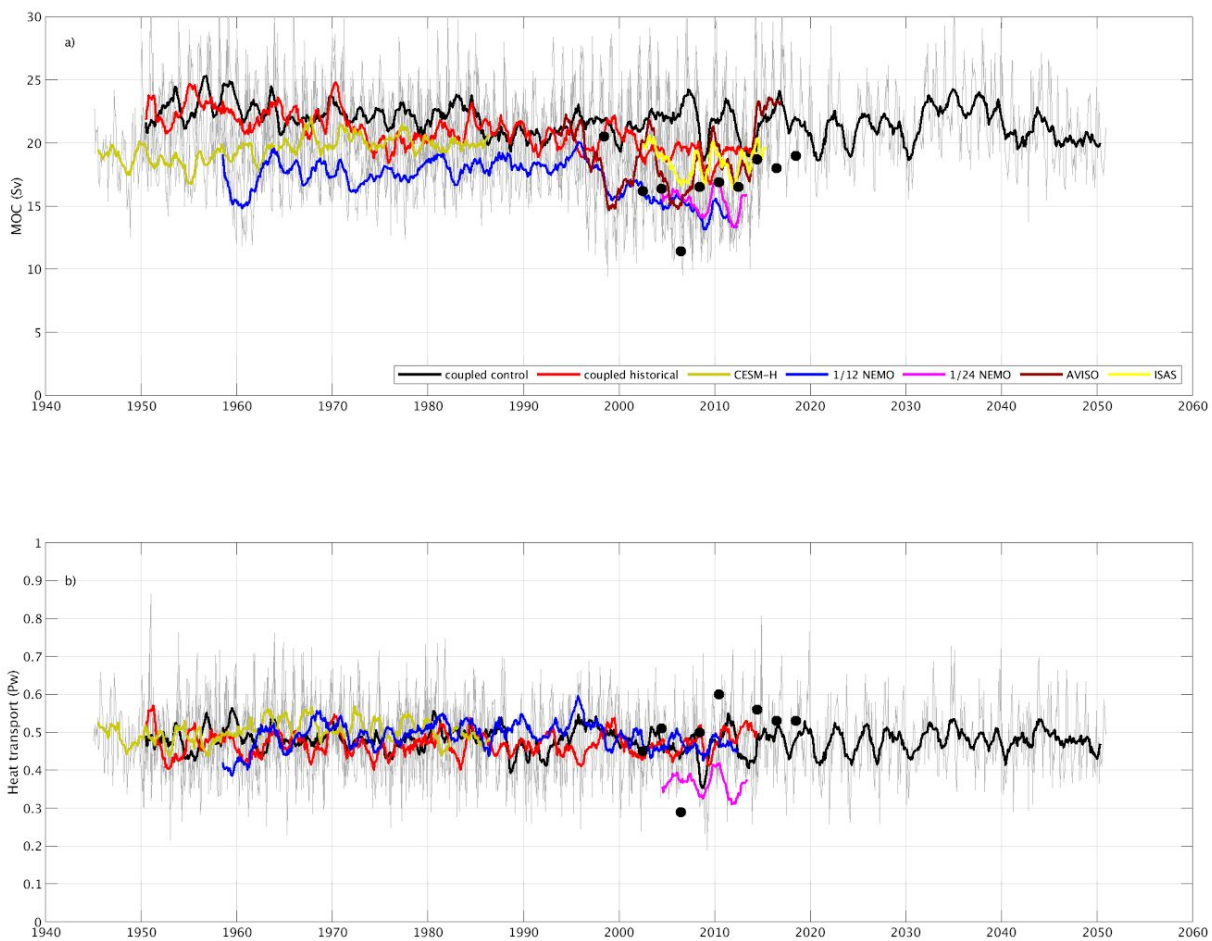


**Figure 4.** Evaluation of model AMOC and heat transports at the OVIDE section. Symbols indicate the bi-annual cruise estimates.

The AMOC at OVIDE is 20 to 22 Sv in the coupled simulations, 2 to 3 Sv higher than that predicted by the ISAS and AVISO estimates. The hindcast models NEMO12 and NEMO24 are lower in the

## Blue-Action Deliverable D2.1

mean than the coupled models. The variability from the ISAS and AVISO estimates are larger than the model prediction. With the exception of the NEMO24 model, the heat transport from other models agree well with each other.

|                    | AMOC<br>(Sv) | Heat transport<br>(PW) |
|--------------------|--------------|------------------------|
| HADGEM3 Control    | 21.74 ± 2.98 | 0.48 ± 0.09            |
| HADGEM3 Historical | 20.85 ± 2.93 | 0.47 ± 0.09            |
| CESM-H             | 20.18 ± 2.68 | 0.51 ± 0.07            |
| NEMO12             | 16.11 ± 2.61 | 0.48 ± 0.07            |
| NEMO24             | 15.38 ± 1.92 | 0.36 ± 0.06            |
| Observation AVISO  | 18.99 ± 4.94 | n/a                    |
| Observation ISAS   | 18.68 ± 4.32 | n/a                    |

**Table 3.** Mean AMOC and heat transport across the OVIDE section. The N06 model is selected after 1993, to correspond as best as possible with the observational data sets.

### 1.5 Evaluation of model transports at the OSNAP section

The OSNAP observing system (Fig. 1) comprises an integrated coast-to-coast array of two sections: OSNAP West, extending from the southeastern Labrador shelf to the southwestern tip of Greenland, and OSNAP East, extending from the southeastern tip of Greenland to the Scottish shelf. The AMOC, heat transport, fresh water transport and freshwater divergence are estimated in the models and evaluated against observations. We have estimated the AMOC and transports of heat into east and west regions, as well as decomposing the east and west regions into overturning and isopycnal transports. At the time of publication only 2 years of the observational OSNAP time series is available.

The AMOC in all three coupled models are typically too high, 21 to 23 Sv, vs 15 Sv from observation (Table 4, Figure 5), which leads to a higher heat transport ( 0.51 to 0.59 PW, vs 0.45 PW from observation). The AMOC in the NEMO12 and NEMO24 models are closer to observation than the coupled models ( 15.1 and 16.9 Sv, vs 14.9 Sv). All models overestimate the variability of the AMOC and the heat transport. With the exception of CESMH, the freshwater divergence estimates from all models are very close to observation (-0.30 Sv to -0.36 Sv, vs -0.33 Sv from observation Table 1). CESMH has a slightly low freshwater transport divergence (-0.16 Sv) due to the high inflow through the Bering Straits (Task 1, Section 1.8).

The model estimates of the AMOC in OSNAP East broadly agrees with observation ( 13.8 Sv to 19.24 Sv, vs 15.56 Sv from observation (Table 5, Figure 6). All three coupled models also produce similar levels of variability. The OSNAP West section is not estimated as well as the East. Coupled model

## Blue-Action Deliverable D2.1

estimates of the AMOC are typically too high and have too much variability. This probably reflects a strong Labrador Sea water production in the models. Heat transport in both OSNAP West and East are too large (within 0.04PW/0.08PW West/East of observation). Encouragingly the NEMO12 and NEMO24 models both reproduce the OSNAP West and East AMOC and heat transport well (within 0.01 PW (West) and 0.05 PW (East) ). There is a mistake in the overturning heat transport calculation in the west from the CESMH model ( Figure 6f ) which has not been traced at the time of publication.

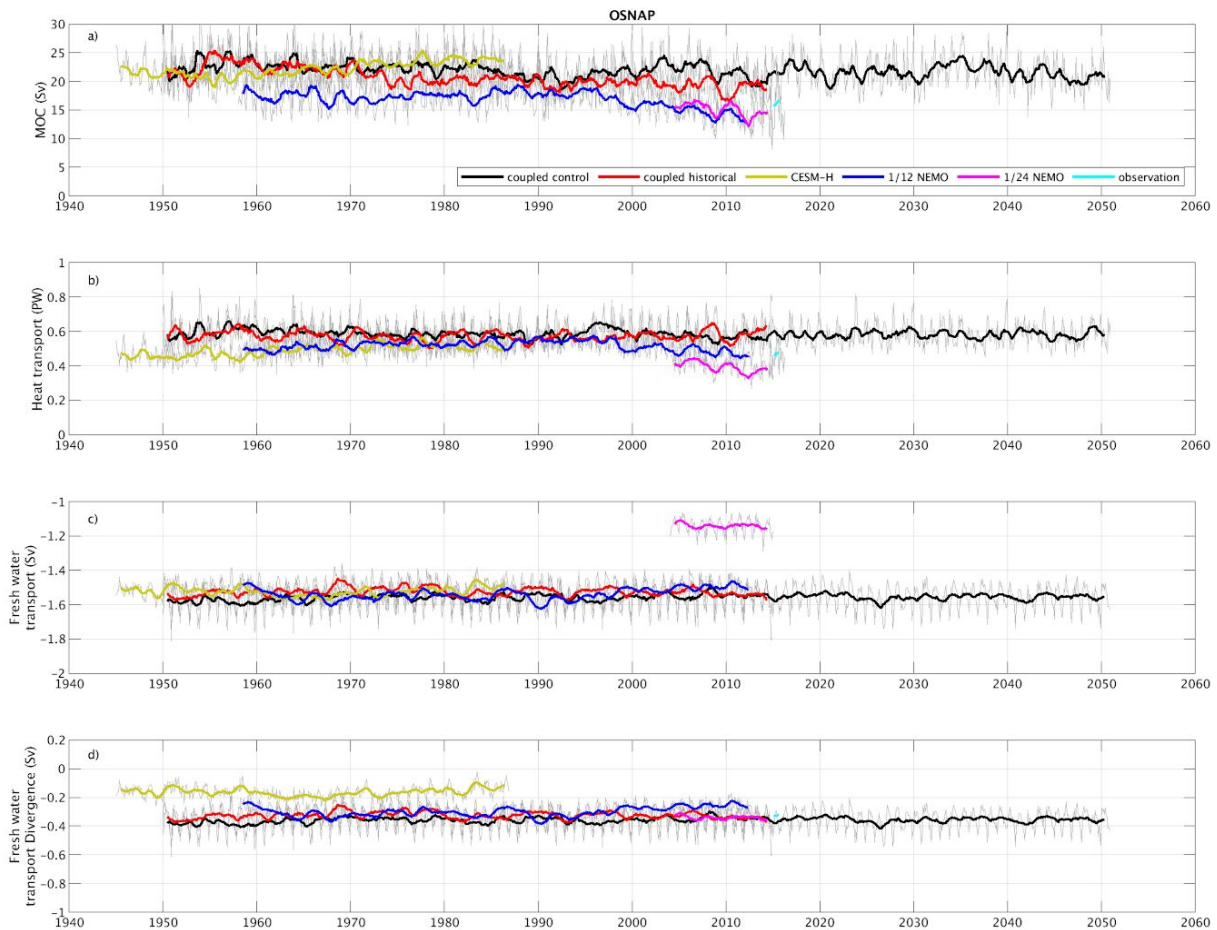


**Figure 5.** The AMOC calculated in density space across the OSNAP section, heat transport and the Freshwater transport from the various models are evaluated against observations.

## Blue-Action Deliverable D2.1

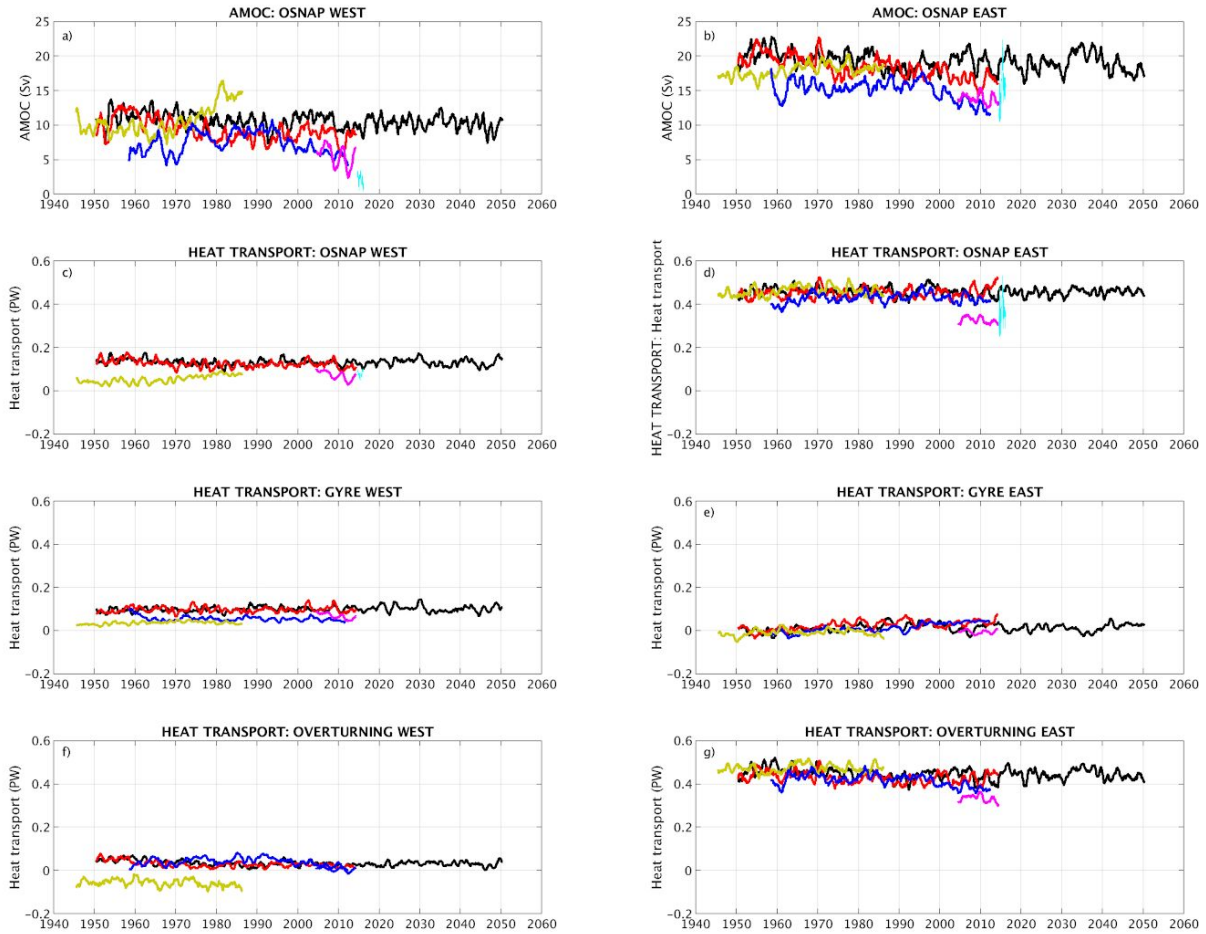


**Figure 6.** The AMOC calculated in density space across the OSNAP West and East section, heat transport and the Freshwater transport from the various models are evaluated against observations.

**Blue-Action Deliverable D2.1**

|                                      | AMOC<br>(Sv) | Heat transport<br>(PW) | Freshwater<br>Transport<br>(Sv) | Freshwater<br>Transport<br>divergence<br>(Sv) |
|--------------------------------------|--------------|------------------------|---------------------------------|---|
| HADGEM3<br>Control                   | 21.90 ± 2.87 | 0.59 ± 0.066           | -1.56 ± 0.070                   | -0.36 ± 0.070                                 |
| HADGEM3<br>Historical                | 20.66 ± 2.92 | 0.57 ± 0.071           | -1.53 ± 0.071                   | -0.32 ± 0.071                                 |
| CESM-H                               | 23.20 ± 2.36 | 0.51 ± 0.051           | -1.52 ± 0.043                   | -0.16 ± 0.043                                 |
| NEMO12                               | 16.85 ± 2.60 | 0.52 ± 0.053           | -1.54 ± 0.053                   | -0.30 ± 0.053                                 |
| NEMO24                               | 15.09 ± 2.17 | 0.39 ± 0.049           | -1.14 ± 0.045                   | -0.34 ± 0.045                                 |
| Observation<br>(Lozier et al., 2019) | 14.9 ± 0.9   | 0.45 ± 0.02            | n/a                             | -0.33 ± 0.01                                  |

**Table 4.** The mean AMOC, transports of heat and freshwater, and the freshwater divergence at the OSNAP section. The means for the NEMO12 and NEMO24 hindcast simulation are for the OSNAP period only.

|      |               | HADGEM3<br>Control | HADGEM3<br>Historical | CESM-H      | NEMO12     | NEMO24      | observation |
|------|---------------|--------------------|-----------------------|-------------|------------|-------------|-------------|
| WEST | AMOC          | 10.56±2.67         | 9.27±2.71             | 11.90±3.74  | 7.32±2.61  | 5.56±2.33   | 2.10±0.92   |
|      | HT            | 0.13±0.032         | 0.12±0.034            | 0.07±0.030  | 0.09±0.031 | 0.07±0.027  | 0.08±0.016  |
|      | ISOPYC<br>NAL | 0.10±0.039         | 0.10±0.036            | 0.04±0.013  | 0.05±0.018 | 0.07±0.018  | n/a         |
|      | OVER          | 0.03±0.040         | 0.03±0.039            | -0.06±0.054 | 0.04±0.032 | 0.01±0.02   | n/a         |
| EAST | AMOC          | 19.24±3.13         | 18.36±3.02            | 18.46±3.02  | 15.08±2.54 | 13.83±1.81  | 15.56±3.1   |
|      | HT            | 0.46±0.054         | 0.45±0.058            | 0.47±0.053  | 0.43±0.044 | 0.43±0.044  | 0.38±0.076  |
|      | ISOPYC<br>NAL | 0.01±0.032         | 0.02±0.034            | -0.01±0.028 | 0.01±0.026 | -0.006±0.02 | n/a         |
|      | OVER          | 0.45±0.051         | 0.43±0.052            | 0.47±0.047  | 0.42±0.046 | 0.33±0.038  | n/a         |

**Table 5.** The mean AMOC and heat transport in the eastern and western region of the OSNAP section. The heat transport is further decomposed into overturning and isopycnal components.

**1.6 Evaluation of model transports at the Greenland Scotland Ridge (GSR)**

The Greenland Scotland Ridge (GSR) is the main pathway for exchange of deep water masses between the Nordic Seas and the North Atlantic, which forms an essential part of the Meridional Overturning Circulation. Oceanic heat transport across the GSR is a key component of the climate system which has to be modelled correctly to be able to predict future Arctic Ocean sea ice changes and variability in European Climate.

Observational volume transports are provided by Blue Action Partners in WP2 D2.8 (Østerhus et al, 2019). It consists of the sum of the Iceland-Faroe Ridge, Denmark Strait and Faroe Shetland Channel Inflows, and the Southward Denmark Strait and Faroe-Bank Channel overflows. Model time series of volume and temperature transport and the average transports are shown in Figure 7 and Table 6.

Volume transports estimates from the coupled climate models are generally within 0.2 Sv of the observations. The hindcast ocean only models have a similar transport magnitude, but have a southwards net transport. Typically the models reproduce the temperature transports to within 0.04 PW, with similar variability to observation. The NEMO24 model is slightly lower at 0.18 PW (0.07 PW less than observation).

|                                       | Volume transport (Sv) | Temperature Transport (PW) |
|---------------------------------------|-----------------------|----------------------------|
| HADGEM3 Control                       | 0.45 ± 1.10           | 0.27 ± 0.04                |
| HADGEM3 Historical                    | 0.25 ± 1.07           | 0.26 ± 0.05                |
| CESM-H                                | 0.08 ± 1.01           | 0.29 ± 0.04                |
| NEMO12                                | -0.23 ± 0.94          | 0.23 ± 0.04                |
| NEMO24                                | -0.44 ± 0.74          | 0.18 ± 0.03                |
| Observation<br>(Østerhus et al, 2019) | 0.2                   | 0.25 ± 0.05                |

**Table 6.** Mean volume and temperature transports across the Greenland Scotland Ridge.

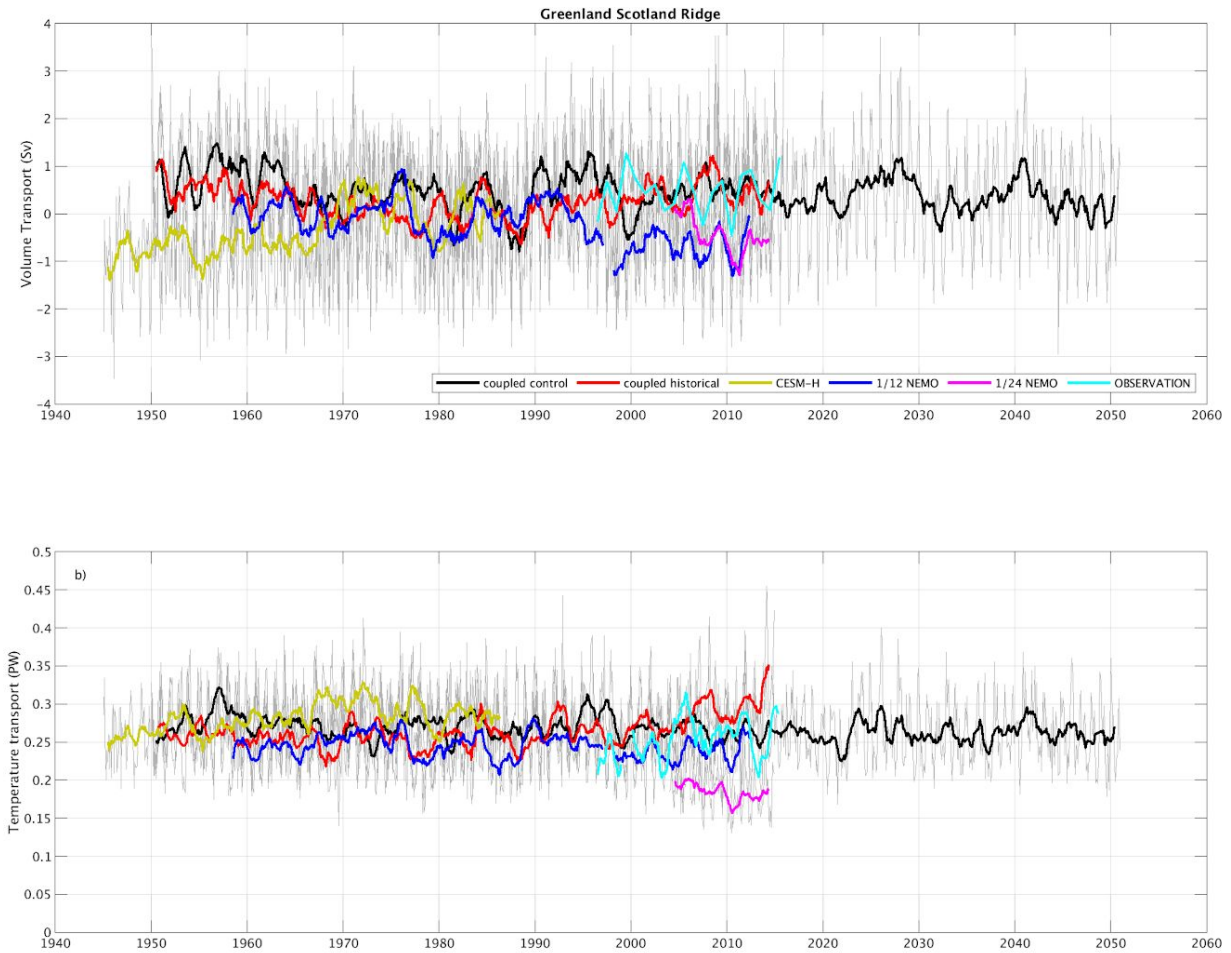


**Figure 7.** Volume and temperature transports across the Greenland Scotland Ridge from model and observation.

### 1.7 Evaluation of model transports at the Davis Strait

The Davis Strait is a primary gateway for the exchange of water mass from the Arctic to the North Atlantic. Observational estimates between 2004 and 2010 show that heat is transported northwards ( $23.28 \pm 12.23$  TW) towards the Arctic and volume ( $-1.66 \pm 0.72$  Sv) is transported southwards out of the Arctic region (Curry et al. 2014). The two HADGEM3 models have strong volume transports which give rise to larger temperature and salinity transports than those observed (table 7 and Figure 8). The CESMH model reproduces the transports well. The NEMO 12 model has a reasonable volume transport, but has weak temperature structure and high salinity structure. The NEMO 24 model has weaker transports across the Davis Strait.

Blue-Action Deliverable D2.1

|                                    | Volume transport (Sv) | Temperature Transport (TW) | salinity transport (Sv psu) |
|------------------------------------|-----------------------|----------------------------|-----------------------------|
| HADGEM3 Control                    | $-2.3 \pm 0.71$       | $31.12 \pm 15.64$          | $-77.73 \pm 24.45$          |
| HADGEM3 Historical                 | $-2.1 \pm 0.67$       | $29.38 \pm 14.41$          | $-69.98 \pm 23.02$          |
| CESM-H                             | $-1.72 \pm 0.72$      | $19.82 \pm 11.30$          | $-56.40 \pm 24.36$          |
| NEMO12                             | $-1.89 \pm 0.69$      | $11.06 \pm 10.03$          | $-61.45 \pm 23.24$          |
| NEMO24                             | $-1.19 \pm 0.56$      | $12.83 \pm 8.58$           | $-39.32 \pm 18.91$          |
| Observation<br>(Curry et al, 2014) | $-1.66 \pm 0.72$      | $23.28 \pm 12.23$          | $-54.51 \pm 24.65$          |

**Table 7.** Mean volume, temperature and salinity transports across the Davis Strait.

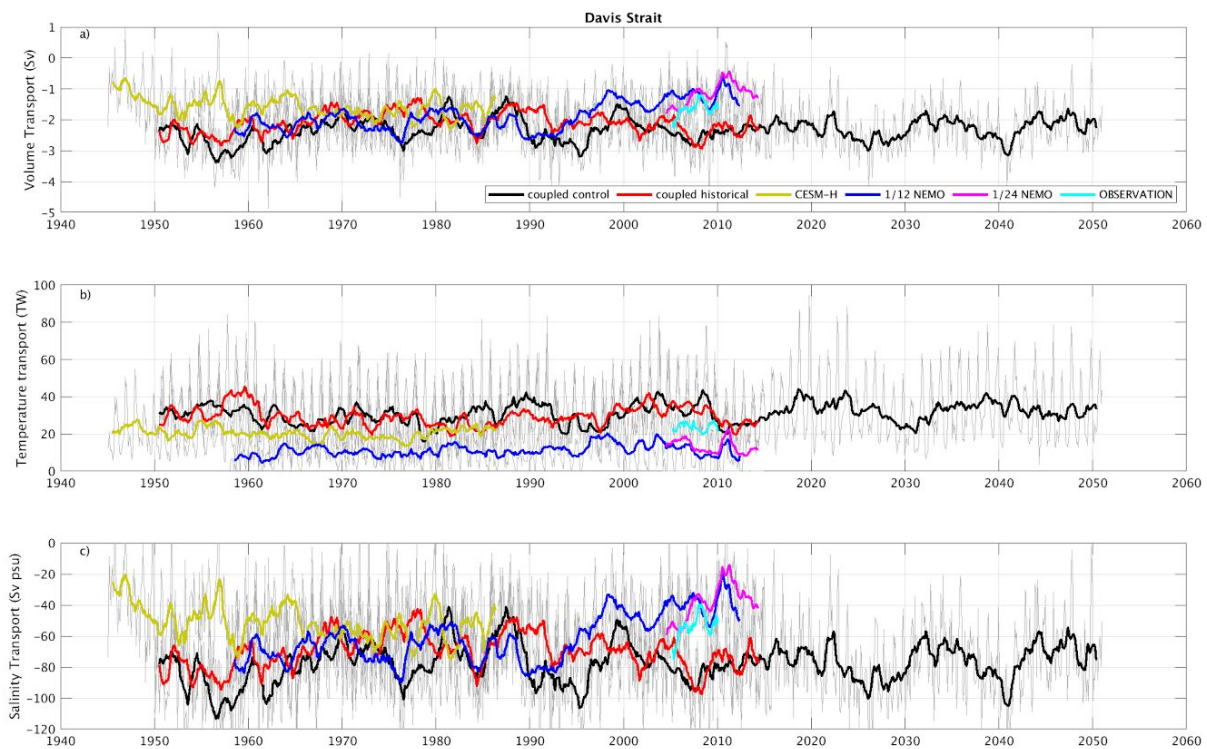


**Figure 8.** Volume, temperature and salinity transports across the **Davis Strait** from model and observation.

### 1.8 Evaluation of model transports at the Bering Strait

The Bering Straits is the main water pathway for freshwater to enter the Arctic ocean. Accuracy in model prediction is crucial in calculating the transport of freshwater in the Atlantic Ocean. The Bering Strait transports of volume, temperature and salinity are compared with observations made by the University of Washington, USA (Woodgate et al., 2018). The time series are shown in Figure 9 and the mean transports and basin average salinity are shown in Table 8. The volume transports from the coupled models are typically too strong ( 1.20 to 1.36 Sv ) when compared to observation (0.95 Sv), but the mean salinity across the section is within about 0.06 psu of observation for the HADGEM models. CESM-H has lower basin mean salinity than the other coupled models, but when combined with a strong volume transport gives rise to a strong salinity transport. The ocean only NEMO12 and NEMO24 models have low basin mean salinities. The NEMO24 model has a lower than observation volume transport which lead to a weak salinity transport. The temperature transport variability in the models is greater than that observed. The models generally have larger variability in the transports than observation. The volume transports across the Bering Strait are used in the freshwater transport divergence calculations.

|  | Volume Transport<br>(Sv) | Salinity transport<br>(Sv psu) | Temperature transport<br>(TW) | mean salinity<br>(psu) |
|--|--------------------------|--------------------------------|-------------------------------|------------------------|
| HADGEM3<br>Control                       | 1.24 ± 0.60              | 40.24 ± 19.34                  | 4.13 ± 15.25                  | 32.5347                |
| HADGEM3<br>Historical                    | 1.20 ± 0.60              | 39.85 ± 19.45                  | 4.23 ± 14.87                  | 32.4842                |
| CESM-H                                   | 1.36 ± 0.61              | 43.34 ± 19.25                  | 9.35 ± 18.82                  | 31.3442                |
| NEMO12                                   | 1.23 ± 0.42              | 39.80 ± 13.77                  | 5.64 ± 14.56                  | 32.1175                |
| NEMO24                                   | 0.88 ± 0.35              | 28.36 ± 11.36                  | 4.38 ± 12.50                  | 32.0032                |
| Observation<br>( Woodgate et al., 2018 ) | 0.95 ± 0.44              | 30.71 ± 14.15                  | 0.78 ± 8.01                   | 32.4713                |

**Table 8.** Mean Bering Strait Transports from the various models and observation .

## Blue-Action Deliverable D2.1

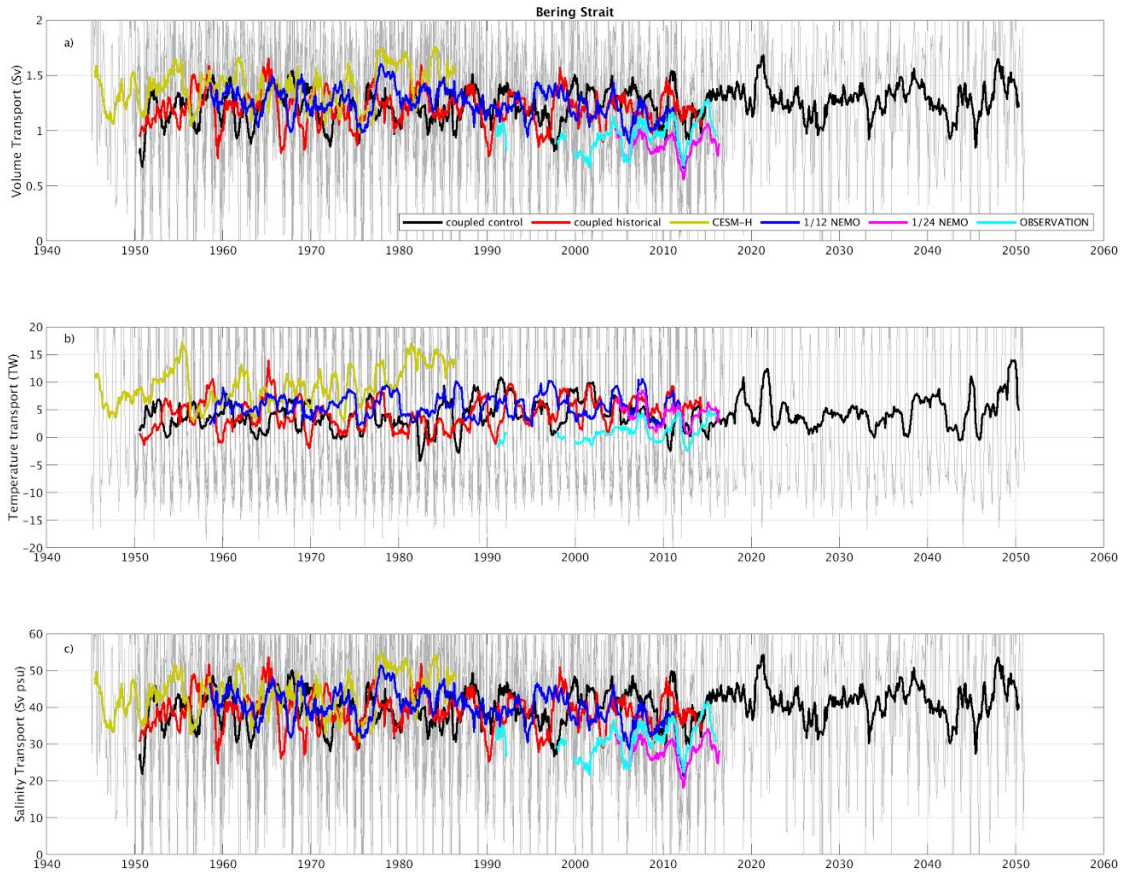


**Figure 9.** Volume, temperature and salinity transports across the Bering Strait from model and observation.

### 1.9 Freshwater transports across the combined Davis Strait and GSR

To enable the estimation of the freshwater transports out of the Arctic the Davis Strait and the Greenland-Scotland ridge have been combined and the salinity has been balanced (See Section 1.2).

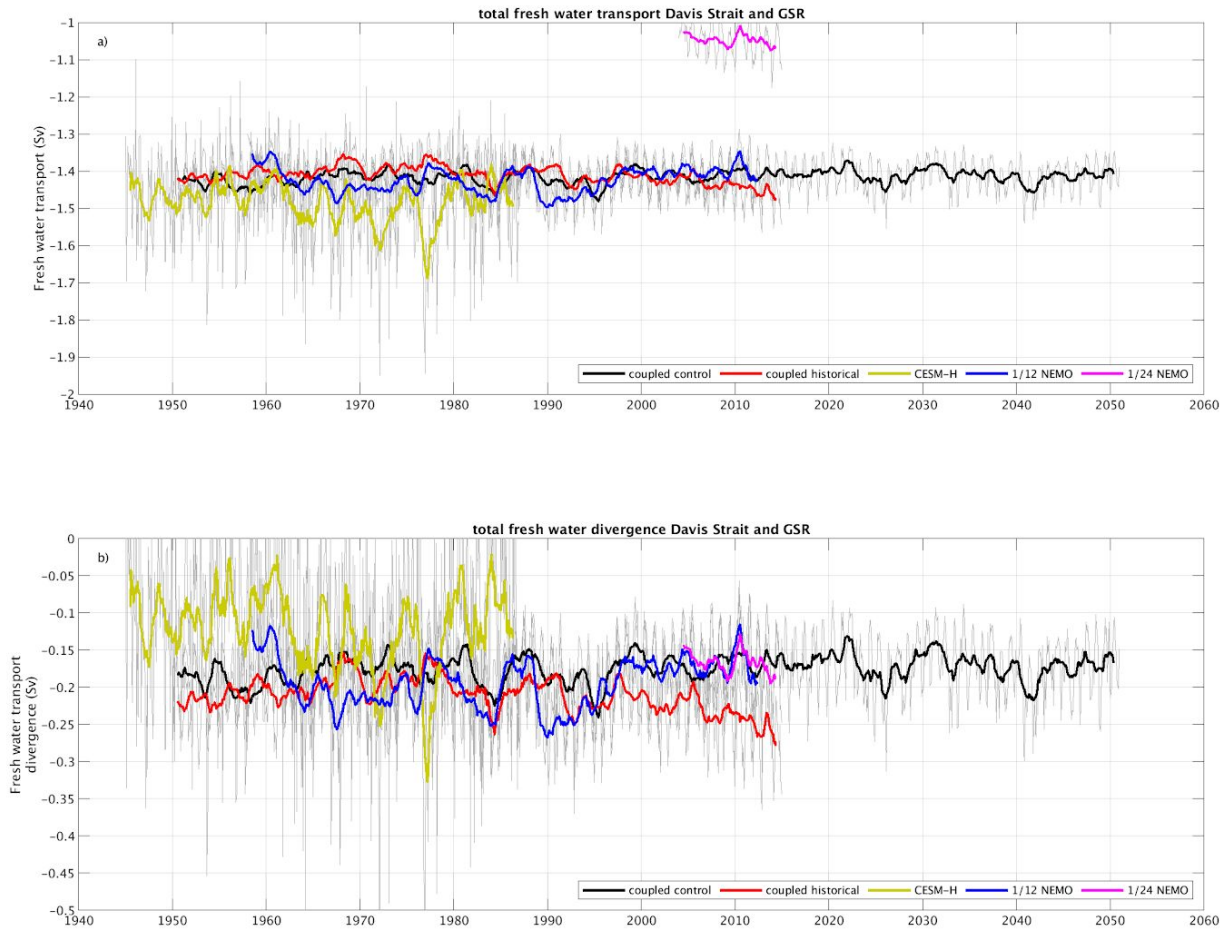


**Figure 10.** Freshwater transport at the combined Davis Strait and Greenland Scotland Ridge, and freshwater transport divergence from the Bering Straits.

|                    | total fresh water transport<br>(Sv) | fresh water transport<br>divergence<br>(Sv) |
|--------------------|-------------------------------------|---|
| HADGEM3 Control    | -1.42 ± 0.042                       | -0.18 ± 0.042                               |
| HADGEM3 Historical | -1.41 ± 0.048                       | -0.21 ± 0.048                               |
| CESM-H             | -1.49 ± 0.14                        | -0.13 ± 0.14                                |
| NEMO12             | -1.42 ± 0.054                       | -0.19 ± 0.054                               |
| NEMO24             | -1.05 ± 0.046                       | -0.17 ± 0.046                               |

**Table 9.** Mean freshwater transports across the combined **Davis Strait and Greenland Scotland Ridge** from the various models.

**Partner contributions**

NERC/NOC: Ben Moat, Penny Holliday, Bablu Sinha, Simon Josey. Provided RAPID 26°N and OSNAP observational data. Provided NEMO 1/12 degree model hindcast data.

University of Washington: Craig Lee and Rebecca Woodgate. Provided Davis Strait and Bering Strait observational transport time series.

HAV, MSS, MRI: Karin Margretha Larsen, Bogi Hansen, Barbara Berx, Hedinn Valdimarsson. Greenland Scotland Ridge observational time series.

CNRS: Christophe Herbaut. 1/24 NEMO ocean model data.

NCAR/UCAR/WHOI: Steve Yeager, Justin Small, Young-Oh Kwon, Laura Flemming. Provided CESM-H model data

**Non-partner Contributions**

IFREMER: Herle Mercier. Provided OVIDE AMOC time series and heat transports.

BSH: Kerstin Jochumsen. Greenland Scotland Ridge observational time series.

**2. Completion of in-situ ocean data (TMA dn GO-SHIP) with remote sensed data from Argo profiling floats, underwater gliders and satellite data**

**2.1 Argo Float profiles used at the RAPID 26°N Array**

The RAPID transport mooring array at 26°N is complemented by Argo float profiles to enable the estimation of the oceanic transports of heat and freshwater between Africa and the Bahamas. An optimal interpolation (OI) method mapping on density surfaces was used to create temperature and salinity fields between 2004 and 2017 (Figure 11). The mooring temperature and salinity measurements from the RAPID array moorings were also assimilated into the OI fields. The OI method has previously been used to provide 3-D gridded fields for ( Johns et al, 2011 ; Desbruyeres, et. al. , 2014; McDonagh et al. 2015; and Desbruyeres, et. al. , 2017 ).

The resulting temperature and salinity fields were used to update the latest time series of heat and freshwater at 26°N to February 2017 (for methods see: Johns et al, 2011 and McDonagh et al. 2015). Heat transport time series and it's components can be obtained from <https://mocha.rsmas.miami.edu/mocha/index.html>. The freshwater transport time series will be released in 2020. These updated time series of heat and freshwater at 26°N in the North Atlantic are included in Bryden et al. 2019.

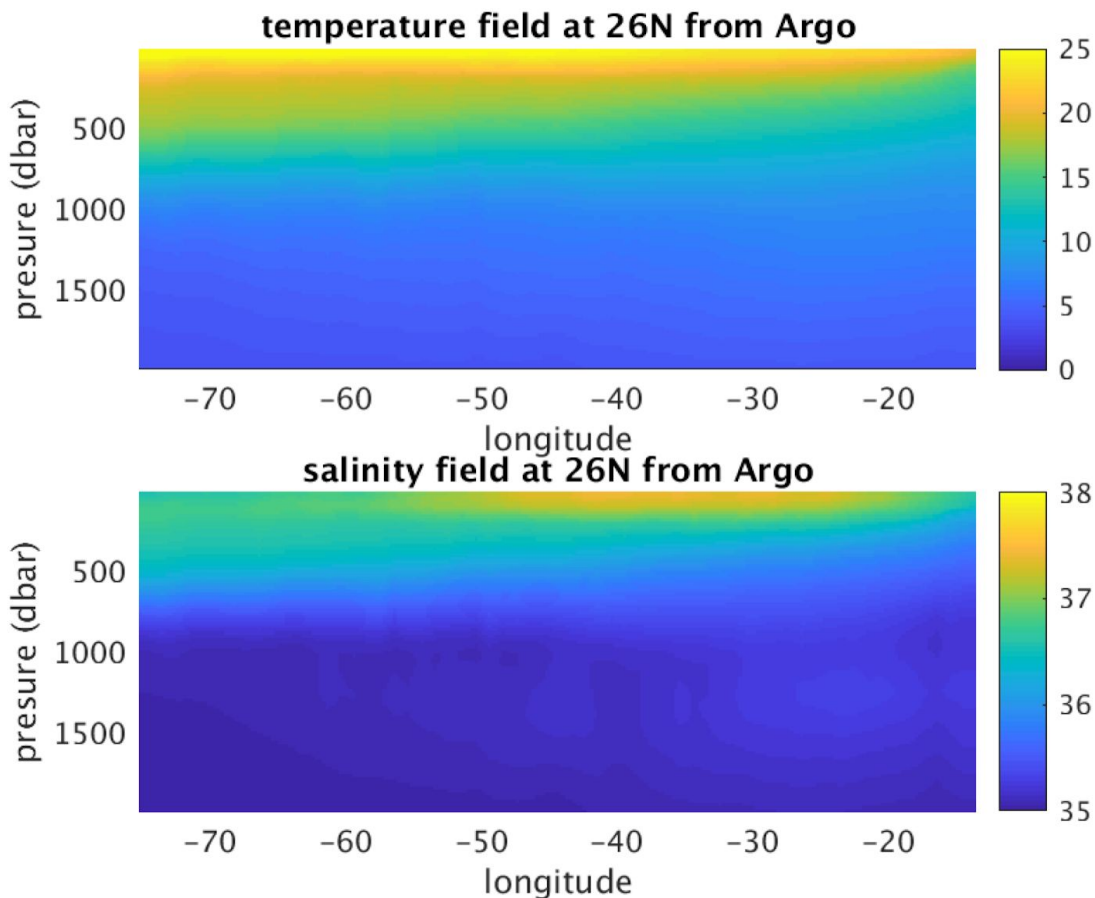


**Figure 11.** Mean Argo OI fields of temperature and Salinity at 26°N in the subtropical North Atlantic between Africa and the Bahamas. This is an average over the period 2004 to 2017.

## 2.2 Ocean glider and Altimetry at OSNAP

Ocean gliders are used as a component of trans-oceanic AMOC observing system to monitor the North Atlantic Current [Houpert *et al.*, 2018; Lozier *et al.*, 2017]. Gliders are autonomous vehicles which perform vertical profiles by changing their buoyancy and move horizontally due to the lift provided by their wings. They complement other in-situ observing platforms (research vessels, Argo floats, Drifters, Mooring network) by covering scales from 1,000 km down to the microscale, and timescales from years to minutes [Liblik *et al.*, 2016]. Over the last decade, gliders were especially useful to observe: i) the coastal/open ocean transition zone, ii) ocean's boundary currents, iii) water mass transformation regions, iv) polar regions, v) mesoscale and submesoscale structures, vi) internal wave and turbulence, vii) biological/biogeochemical processes [Testor *et al.*, 2019].

Gliders move vertically in the water column by changing their buoyancy and achieve vertical speeds of 10-20 cm.s<sup>-1</sup>. Thanks to their wings and their pitch controlled by movable internal battery packs, gliders follow sawtooth paths through the water, moving with a typical horizontal speed of 20-30

## Blue-Action Deliverable D2.1

$\text{cm}\cdot\text{s}^{-1}$ . Standard gliders can profile from the surface to 1000 m, and recently deep glider models can profile up to 6000m. When profiling to 1000 m, a dive cycle takes about 4-6h and the glider travels about 4-6km. The relative low-energy needed by buoyancy-driven gliders make them suitable for long-endurance missions lasting several months and covering thousands of kilometres. Over each dive cycle, the depth-average current (DAC) can be calculated by differencing the horizontal displacement estimated from a hydrodynamic model from the actual glider displacement derived from GPS positions. The DAC accuracy is within  $1 \text{ cm s}^{-1}$  for a glider with stable flight characteristics.

Thanks to their direct measure of the DAC, gliders produce absolutely referenced geostrophic velocity used to quantify boundary current transports. The absolute across-track velocity is calculated from the geostrophic shear by integrating the thermal wind balance, and by considering that the depth-average velocity is equal to the DAC measured by the glider.

Repeat glider sections obtained during 2014–2016, as part of the Overturning in the Subpolar North Atlantic Program (OSNAP), are used to quantify the circulation and transport of North Atlantic Current (NAC) branches over the Rockall Plateau [Houper et al., 2018]. Using 16 glider sections collected along 58N and between 21W and 15 W, absolute geostrophic velocities are calculated by referencing the geostrophic shear to the Depth Average Current measured by the glider during a dive cycle. The annual mean northward transport ( $\pm$  standard deviation) is  $5.1 \pm 3.2 \text{ Sv}$  over the Rockall Plateau. During summer (May to October), the mean northward transport is stronger and reaches  $6.7 \pm 2.6 \text{ Sv}$ . This accounts for 43% of the total NAC transport of upper-ocean waters ( $\sigma_\theta < 27.55 \text{ kg/m}^3$ ) estimated by Sarafanov et al. (2012) along 59.5N, between the Reykjanes Ridge and Scotland. Two quasi-permanent northward flowing branches of the NAC are identified (Figure 12): (i) the Hatton Bank Jet ( $6.3 \pm 2.1 \text{ Sv}$ ) over the eastern flank of the Iceland Basin ( $20.5^\circ\text{W}$  to  $18.5^\circ\text{W}$ ) and (ii) the Rockall Bank Jet ( $1.5 \pm 0.7 \text{ Sv}$ ) over the eastern flank of the Hatton-Rockall Basin ( $16^\circ\text{W}$  to  $15^\circ\text{W}$ ). Transport associated with the Rockall Bank Jet is mostly depth independent during summer, while 30% of the Hatton Bank Jet transport is due to vertical geostrophic shear. Uncertainties are estimated for each individual glider section using a Monte Carlo approach, and mean uncertainties of the absolute transport are less than  $0.5 \text{ Sv}$ .

To compare their glider-based transport estimate to an altimetry-based estimate, Houper et al., [2018] used delayed time gridded data from the SSALTO/DUACS (Data Unification and Altimeter Combination System) system (Pujol et al., 2016): daily global absolute sea-surface dynamic topography, absolute geostrophic velocity and geostrophic velocity anomalies (spatial resolution of  $0.25^\circ$ ). These are distributed through The Copernicus Marine and Environment Monitoring Service (<http://marine.copernicus.eu/documents/QUID/CMEMS-SL-QUID-008-032-051.pdf>). This system consists of a homogeneous, inter calibrated time series of sea level anomaly and mean sea level anomaly (combining data from 13 missions). Although comparisons with altimetry-based estimates indicate similar large-scale circulation patterns, altimetry data do not resolve small mesoscale current bands (30km) in the Hatton-Rockall Basin which constitute a non-negligible part of the meridional transport in the eastern subpolar gyre. These results are in agreement with Pujol et al. (2016) who indicated that geostrophic currents estimated by satellite altimetry are underestimated compared to in situ observations; specifically, they demonstrated that the gridded products are not adapted to resolve the small mesoscale. The comparison with the spectral content computed from full-resolution Saral/AltiKa 1-Hz along-track measurements showed that nearly 60% of the energy observed in along-track measurements at wavelengths ranging from 200 to 65 km is missing in the SLA gridded

## Blue-Action Deliverable D2.1

products. Thus, the mapping methodology combined with altimeter constellation sampling capability appear to be one of the main reasons why the small mesoscale current bands in the Hatton-Rockall Basin are not resolved in gridded altimetry product.

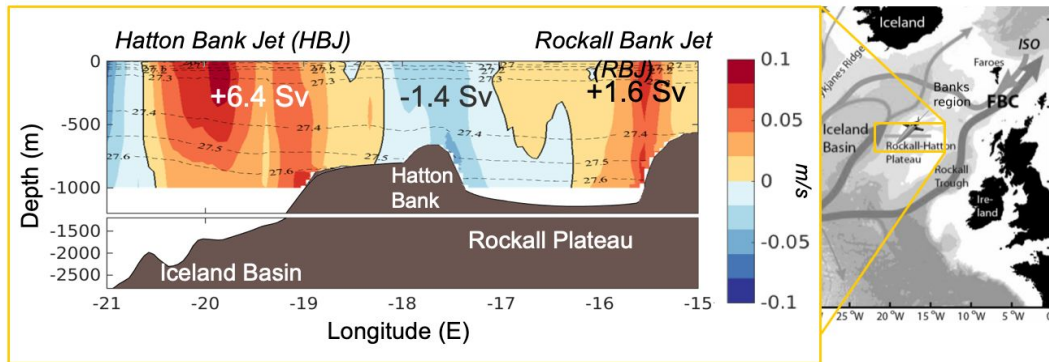


**Figure 12.** Mean absolute meridional geostrophic velocity (m/s) referenced to glider depth-average current. Mean value of the 3 main current branch is indicated on top.

### 2.3 Recreating the AMOC at 26°N using Altimetry

Here we develop a proxy for the AMOC strength, using RAPID mooring data, sea level anomaly (SLA), and ocean bottom pressure (BP). The altimetry from CMEMS uses the following platforms: Envisat, Geosat Follow On, Jason-1, Topex/Poseidon Interleaved. The satellite altimetry and gravimetry datasets were gridded to 0.5 degrees and monthly. The content has been withheld as it is in preparation for Geophysical Research Letters and is in preparation.

Sanchez-Franks, A, E. Frajka-Williams, B. Moat, 2020, Full depth Transport Estimates of the Atlantic Overturning at 26°N from Altimetry and GRACE, Geophysical Research Letters, (in prep).

### 2.4 Altimetry at the Greenland Scotland Ridge

Most of the oceanic heat transport into the Arctic is carried by Atlantic water crossing the Greenland-Scotland Ridge, mainly east of Iceland (Østerhus et al., 2019). The two main Atlantic inflow branches (IF-inflow and FSC-inflow, Figure 13) have been monitored by in situ observations since the late 1990s, combining data from moored ADCPs with CTD data from regular occupations at standard stations, but including altimetry has been found to improve the accuracy of temporal transport variations both for the FSC-inflow (Berk et al., 2013) and for the IF-inflow (Hansen et al., 2015).

## Blue-Action Deliverable D2.1

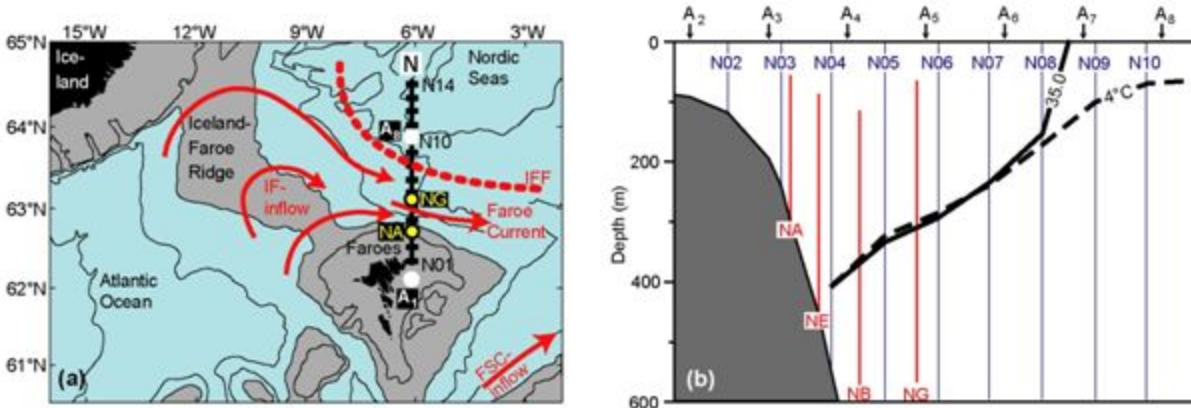


**Figure 13** (a) Red arrows indicate the two main Atlantic inflow branches to the Nordic Seas. The thick black line is the monitoring section. Black rectangles labelled N01 to N14 indicate standard CTD stations. Yellow circles labelled NA and NG indicate two of the long-term ADCP mooring sites. White circles labelled  $A_1$  and  $A_8$  indicate the southernmost and northernmost altimetry grid points selected. (b) The monitoring section with standard CTD stations (blue lines), long-term ADCP mooring sites (red lines labelled NA, NE, NB, and NG), and altimetry grid points  $A_2$  to  $A_8$ . The black lines indicate average locations of the 4°C isotherm (dashed) and the 35.0 isohaline (continuous) used as lower boundary for the Atlantic water on the section.

In Blue-Action, the use of altimetry for transport monitoring has been evaluated in more detail for the IF-inflow, which is monitored on a section where the flow has been focused into the Faroe Current (Figure 13). The satellite data used are from Copernicus Marine Environment Monitoring Service (product SEALEVEL\_GLO\_PHY\_L4\_REP\_OBSERVATIONS\_008\_047, including new missions data from Jason-3 and Sentinel-3A). Correlations between sea level change from one altimetry grid point to another and surface velocity extrapolated from ADCP profiles in between were not found to be very high. A linear combination of surface velocities from the four long-term ADCP sites covering the current core was, however, found to be highly correlated with the sea level difference between the altimetry grid points spanning the region ( $A_3$  and  $A_5$ , Figure 13b,  $R = 0.86$ ,  $p < 0.001$  for 94 contiguous 28-day averages, Hansen et al., 2019a).

This result illustrates the fact that the surface velocity derived from altimetry is horizontally averaged, which can make it better suited for integration into transport estimates than direct current measurements from moorings even if they are closely spaced. This is, however, only true for the temporal variations of surface velocity. Using the Mean Dynamic Topography from the AVISO+ data set to derive absolute current velocities was found to give a velocity structure that is too smooth horizontally compared to the ADCP data (Hansen et al., 2015). Instead, in situ observations (ADCP + CTD) have been used to calibrate the altimetry data to give less biased surface velocities (Hansen et al., 2019a).

For transport estimates, velocities have to be integrated vertically, but for the Faroe Current at least, the ADCP data show that the vertical structure of the velocity variations is sufficiently consistent

## Blue-Action Deliverable D2.1

so that ≈95% of the variance in the volume transport down to the average depth of the Atlantic layer on monthly time scales may be explained by variations of the surface velocity (Hansen et al., 2019a).

Thus, altimetry seems to be a very suitable tool for monitoring the velocity structure of the Faroe Current both at the surface and at depth, but - as for the other Atlantic inflow branches - water masses of Arctic origin also pass through the monitoring section and need to be distinguished from the Atlantic water. This is usually achieved by using hydrography and for the Faroe Current, the 4°C isotherm is used as a lower boundary for the Atlantic water layer over most of the section (Figure 13b). Fortunately, geostrophic adjustment makes the hydrographic fields respond rapidly to velocity variations (Hansen et al., 2019b).

Variations in the 4°C isotherm depth along the section may therefore also be estimated from altimetry (Hansen et al., 2015), but the accuracy of these estimates is not well known since it has only been evaluated by comparison with snapshot CTD profiles. As part of Blue-Action, two PIES (Pressure Inverted Echo Sounders) have been moored on the monitoring section for more than a year, during which time they are found to allow determination of the 4°C isotherm depth with a high accuracy (Hansen et al., 2019b). The data from these deployments are being processed and will be used to estimate the ability of altimetry to give isotherm depth and hence transport of Atlantic water through the section. The results of this analysis will be reported in deliverable D2.8.

### 2.5 Altimetry at the GO-Ship A25 OVIDE section

The Greenland-Portugal line was occupied since 2002 every other year in the framework of OVIDE (Observatoire de la Variabilité Interannuelle à Décennale) project (Mercier et al. 2015). About ninety hydrographic stations were occupied during each cruise. Ship-mounted Acoustic Doppler Current Profiler (S-ADCP) measurements were combined with hydrography to estimate the absolute transports across the OVIDE line. These transports provided benchmarks for monthly AMOC estimates based on the ISAS gridded product and altimetry (Figure 14) that were combined as explained below.

The monthly In Situ Analysis System (ISAS) provides gridded fields of temperature and salinity over the period 2002–2017 on a square horizontal grid of side equal to  $0.5^\circ \times 0.5^\circ \cos(\text{latitude})$ , on 152 levels in the upper 2000 m (see <http://www.umr-lops.fr/SNO-Argo/Products/ISAS-T-S-fields>). The vertical resolution is 5 m from the surface to 100 m depth, 10 m from 100 m to 800 m depth and 20 m from 800 m to 2000 m depth. The ISAS fields were used to compute the sea surface referenced monthly geostrophic velocities orthogonal to the OVIDE section. The ISAS fields were obtained by optimal interpolation of the large in situ data set provided by the Argo array of profiling floats and complemented by measurements from drifting buoys, CTDs and moorings (Gaillard et al. 2016). For the 1993–1996 time span, we used temperature and salinity fields constructed from objectively analyzed pentadal anomalies down to a depth of 2000 m and associated mean fields (Levitus et al. 2005).

Absolute sea-surface geostrophic velocities orthogonal to the OVIDE section were computed from the absolute dynamic topography, which is the sum of a sea level anomaly (SLA) and a mean dynamic topography (MDT). SLAs were from the multi-mission altimetry products provided by AVISO (gridded delayed time “upd” products) on a  $1/3^\circ$  grid, with data every 7 days since October 1992 and

## Blue-Action Deliverable D2.1

distributed by Copernicus Marine Environment Monitoring Service . We used the 2005 version of the MDT available on a  $1/3^\circ$  grid (Rio 2004).

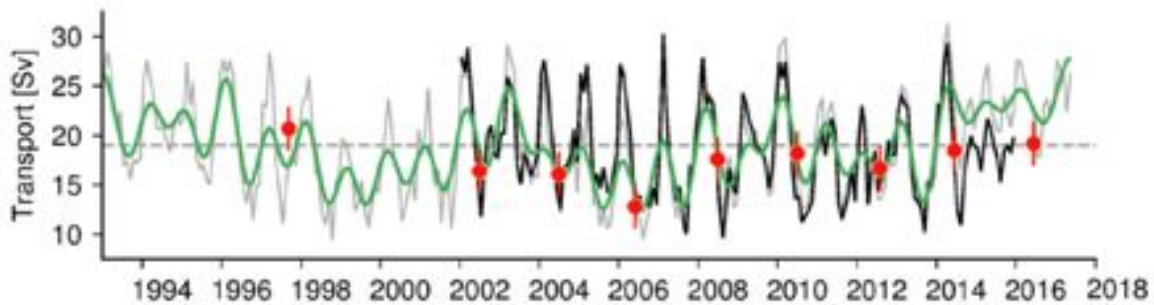


**Figure 14.** A time series of AMOC transport at the OVIDE for 1993–2017, constructed from altimetry and hydrography. The gray line is from altimetry combined with a time-mean of Argo velocities; the green curve is low-pass filtered using a 2-year running mean. The black curve is from altimetry and Argo. Red circles are estimates from OVIDE hydrography with associated errors given by the red lines. The mean of the gray curve is given by the black dashed line.

### Partner Contributions

NERC/NOC: Ben Moat, Alejandra Sanchez-Franks. SAMS: Loic Houpert. Creation of the Argo OI fields. Ocean Glider analysis and altimetry.  
SAMS: Loic Houpert and Stuart Cunningham. Ocean Glider analysis and piloting.  
HAV: Karin Margretha Larsen and Bogi Hansen. Greenland Scotland Ridge Altimetry.

### Non-partner Contributions

IFREMER: Herle Mercier. Altimetry on the OVIDE section.

## 3. Examination of the correspondence between ocean heat transport estimates and atmospheric heat transport in the coupled model simulations

### 3.1 Impact of Arctic climate change on North Atlantic Ocean circulation: a model study

Remote oceanic impacts of Arctic climate change are studied using a 1 degree horizontal resolution surface forced NEMO ocean general circulation model (Madec, 2008). Surface atmospheric fields observed during the Arctic sea ice minimum year 2007 are specified over the Arctic, whilst outside the Arctic observed forcing from 1985 is specified. Relative to a control simulation with 1985 forcing everywhere, modified Arctic forcing causes major changes to the Atlantic Meridional Overturning Circulation (AMOC) and to the temperature, salinity and gyre circulation of the subpolar North Atlantic on timescales of one year to several decades (Figure 15).

A net weakening of the AMOC of  $\sim 10\%$  (Figure 15a, b) results from a combination of reduced deep convection in the ice free regions of the Greenland Sea due to modified surface wind patterns and air-sea heat and freshwater exchange and increased convection in the marginal ice zone of the Greenland Sea due to the retreat of sea ice. Transmission to the Atlantic occurs via propagation of

## Blue-Action Deliverable D2.1

barotropic and baroclinic Kelvin waves along the northern and western boundary of the Atlantic. The wave pathway is visible as a north-south band of anomalously warm SST in the Labrador Sea and over the Gulf Stream extension (Figure 15c). Resulting changes in zonal pressure gradients modify the AMOC. The subpolar response is dominated by a cold anomaly in the central subpolar North Atlantic (Figure 15c) which resembles in some respects a Rossby wave interacting with westward mean flow and ocean bottom topography. Thus changes to Arctic climate may be partially responsible for the North Atlantic Warming Hole.

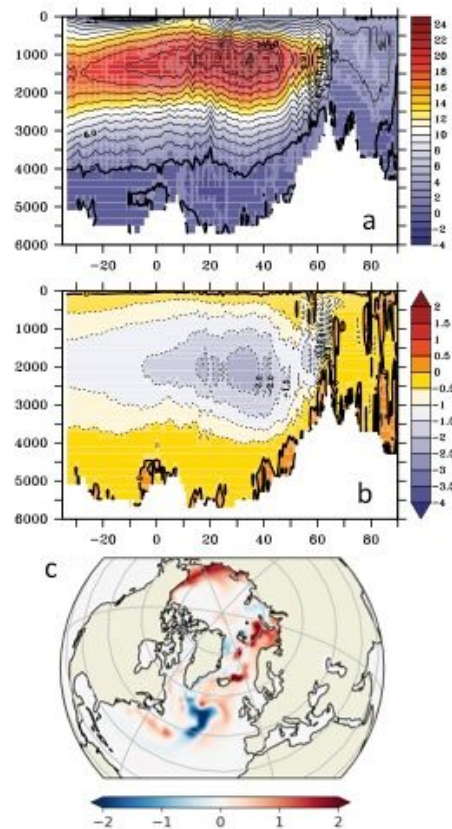


**Figure 15** a) Mean AMOC streamfunction (Sv) for years 31-35 of the control simulation b) mean AMOC streamfunction anomaly (Sv) over the same time period in the simulation with perturbed surface forcing in the Arctic c) Surface temperature anomaly (K, perturbed minus control) due to the changed surface forcing in the Arctic.

In relation to the above:

- A paper has been recently submitted to JGR Oceans, the B. Sinha, B. Topliss, M. Hughes, A. T. Blaker, J. J.-M. Hirschi, C. L. E. Franzke, S. A. Josey, V. Ivchenko, B I Moat, 2019, Impact of Arctic climate change on North Atlantic ocean circulation: a model study, *submitted to JGR-Oceans*.

## Blue-Action Deliverable D2.1

- And a joint paper has been written with the authors of the D2.3 and D2.4: Model output from this Section has contributed to Yang et al. 2019 on atmospheric heat transports, the D2.3 deliverable and D2.4 deliverable. Liu, Yang; Attema, Jisk; Moat, Ben; Hazeleger, Wilco. 2019 [Synthesis and evaluation of historical meridional heat transport from midlatitudes towards the Arctic](https://doi.org/10.5194/esd-2019-17). Earth System Dynamics Discussions. 1-33 <https://doi.org/10.5194/esd-2019-17>

### 3.2 Atmospheric feedbacks in Coupled climate models.

We have investigated the relationship between atmospheric and oceanic heat transports at key locations corresponding to the positions of ocean observational arrays in three state-of-the-art high resolution coupled ocean-atmosphere simulations. The analysis is conducted on two different timescales, interannual-decadal (1-10 years) and multidecadal (>10 years). Here we present results from the interannual timescale analysis.

The correlation of Atlantic ocean heat transport at 26°N with global atmospheric heat transport is shown in Fig 17. Here ocean heat transport is computed from monthly mean ocean meridional velocity and monthly mean ocean potential temperature, whilst global atmospheric heat transport is computed as a residual for top-of-atmosphere and ocean surface net heat flux using the method of Shaffrey and Sutton (2004). A robust response across the model simulations is almost zero correlation between Atlantic ocean heat transport at 26°N and the global atmospheric heat transport directly above. However there is a negative correlation at most other latitudes. The strongest negative correlations occur at ~50N, where there is an anticorrelation reaching as much as -0.5 in the control simulation of HadGEM3-H (the longest of the three simulations) and of slightly lesser magnitude in the HadGEM3.1 historical simulation. CESM-H has a weaker, but still clear maximum anticorrelation closer to 55N. Another region of strong anticorrelation is 10N where the HadGEM3-H historical simulation attains a correlation of -0.4. A further strong negative correlation of -0.4 is seen in the high Arctic, north of 80N in the HadGEM3-H control simulation, but this is weaker in the other two simulations.

We change focus now from global atmospheric heat transport to the regional flow of heat carried by the atmosphere into the Arctic from the North Atlantic in the HadGEM3-H control simulation (Fig 18). We plot the correlation between Atlantic ocean heat transport at 26°N and the northward atmospheric temperature transport  $V_{atm}T_{atm}$ , still at interannual timescales at a latitude of 67N (the latitude of the main oceanic gateways from the Atlantic to the Arctic: Denmark Strait, the Iceland Scotland Ridge, and the Davis Strait). Here  $V_{atm}$  and  $T_{atm}$  are the northwards atmospheric velocity and atmospheric temperature respectively. The other main component of the atmospheric heat transport,  $V_{atm}q_{atm}$  where  $q_{atm}$  is atmospheric specific humidity, behaves similarly to the temperature transport. A very clear signal emerges whereby there is enhanced (reduced) northward atmospheric temperature transport to the east (west) of Greenland when the Atlantic ocean heat transport at 26°N is high. Taking the mean heat transport (not shown) into account, this amounts to an eastward shift in the location of the maximum atmospheric heat transport from the North Atlantic region to the Arctic.

We conclude that changes in both global and regional Atlantic atmospheric heat transport into the Arctic are associated with changes to the subtropical oceanic heat transport on interannual

timescales. It is likely that these changes, in turn are part of a large scale atmospheric mode of variability. Further investigation of this mode of variability and also of impacts on Arctic climate will be investigated in future work.

Preliminary results for the longer timescale multidecadal variability indicate that global atmosphere and Atlantic ocean heat transports are more strongly locally anticorrelated compared with interannual variability (including at 26°N), in other words, the global atmospheric heat transport at each latitude is strongly anticorrelated with the Atlantic ocean heat transport at the same latitude. However further work is required to determine the robustness of this result across the model simulations, its physical mechanism and its implications for Arctic climate variability.

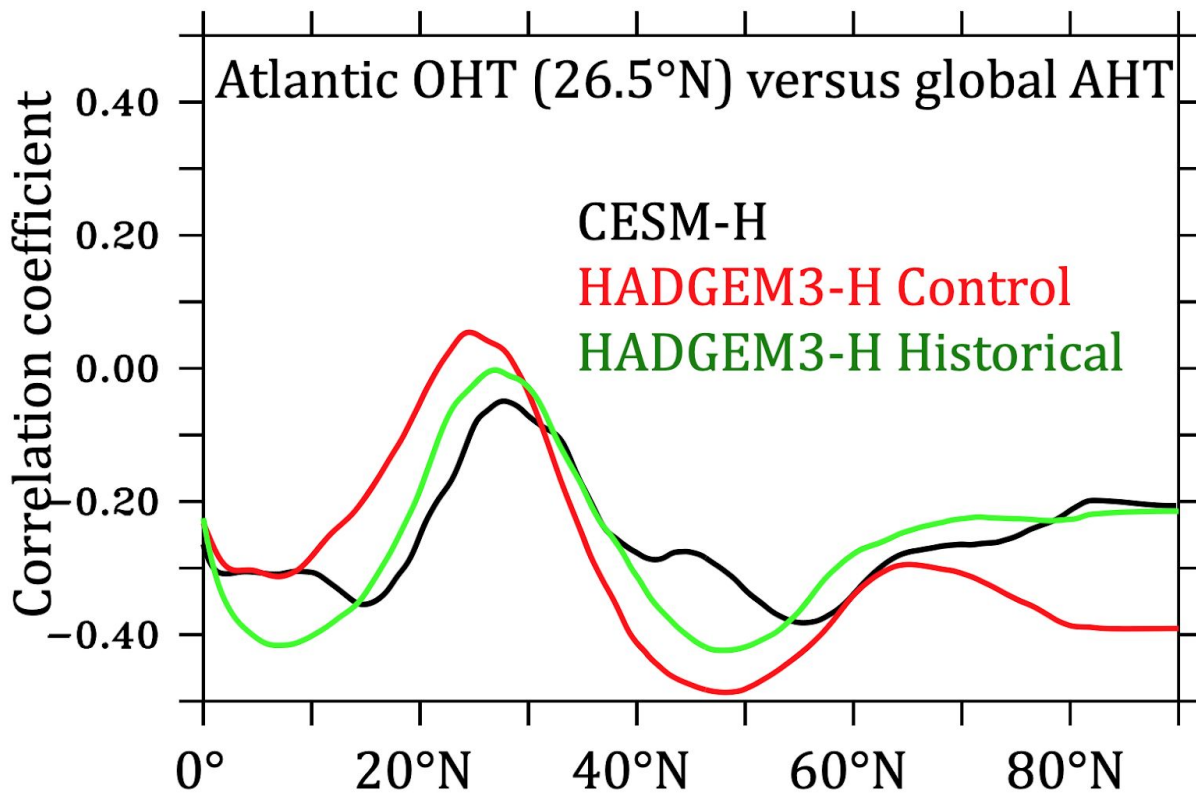


**Figure 16.** Interannual time scale correlations between global atmospheric meridional heat transport (AHT) at different latitudes and ocean meridional heat transport (OHT) in the Atlantic at 26°N. Coloured lines show the results from three different coupled climate model simulations, CESM-H present day control simulation (black), HadGEM3-H 100-year present day control simulation (red) and HadGEM3-H historical simulation, 1950-2015 (green). All time series are based on monthly mean output and have been bandpass filtered to retain 1-10 year timescales.

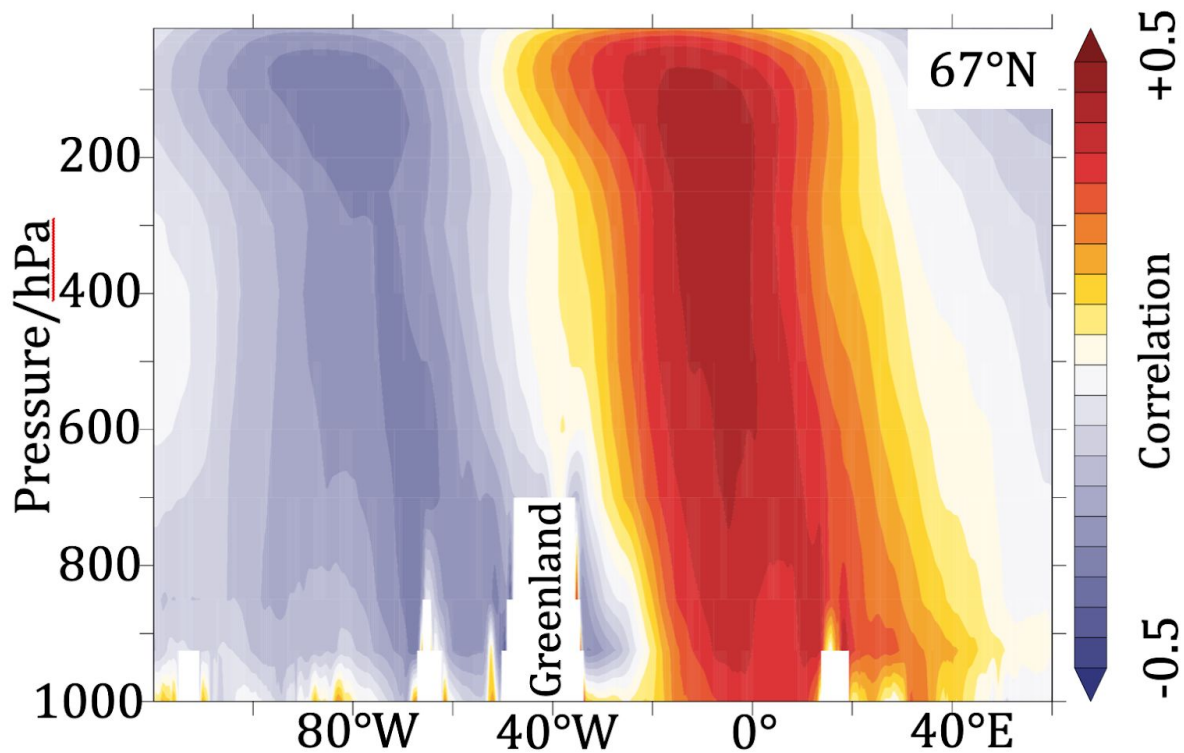


**Figure 17.** Interannual time scale correlations between Atlantic sector atmospheric meridional temperature transport ( $V_{\text{atm}} T_{\text{atm}}$ ) and ocean meridional heat transport in the Atlantic at  $26^{\circ}\text{N}$  as a function of altitude (pressure) and longitude from the HadGEM3-H 100-year present day control simulation. Ocean and atmosphere transports were both calculated directly from ocean velocity temperature data. All time series are based on monthly mean output and have been bandpass filtered to retain 1-10 year timescales. Note that the atmosphere model outputs monthly mean values of  $V_{\text{atm}} T_{\text{atm}}$  in order to include the effects of atmospheric synoptic variability.

#### Partner contributions

NERC/NOC: Bablu Sinha, Ben Moat and Simon Josey. Model creation and Analysis

NLeSC: Liu, Yang, J. Attema and W. Hazeleger. Shared data resources for paper submission.

NCAR/UCAR and WHOI: Steve Yeager, Justin Small, Young-Oh Kwon, and Laura Fleming.

Provided CESM-H model data.

## Main results achieved

### Evaluation of heat and freshwater transport to the Arctic from state-of-the-art coupled climate models

The temperature and heat transports for each of the North Atlantic Sections described in TASK 1 are summaries in Figure 18. The coupled model simulations estimate have too much heat going into the Arctic region and the transports have too much variability. The coupled models do estimate the heat

transport across the RAPID 26°N section well ( 1.3 PW vs, 1.2 PW from observation), but this is due to a higher model AMOC increasing the heat transport rather than the model having an accurate vertical stratification. In general, the high resolution hindcast models tend to underestimate the heat transports.

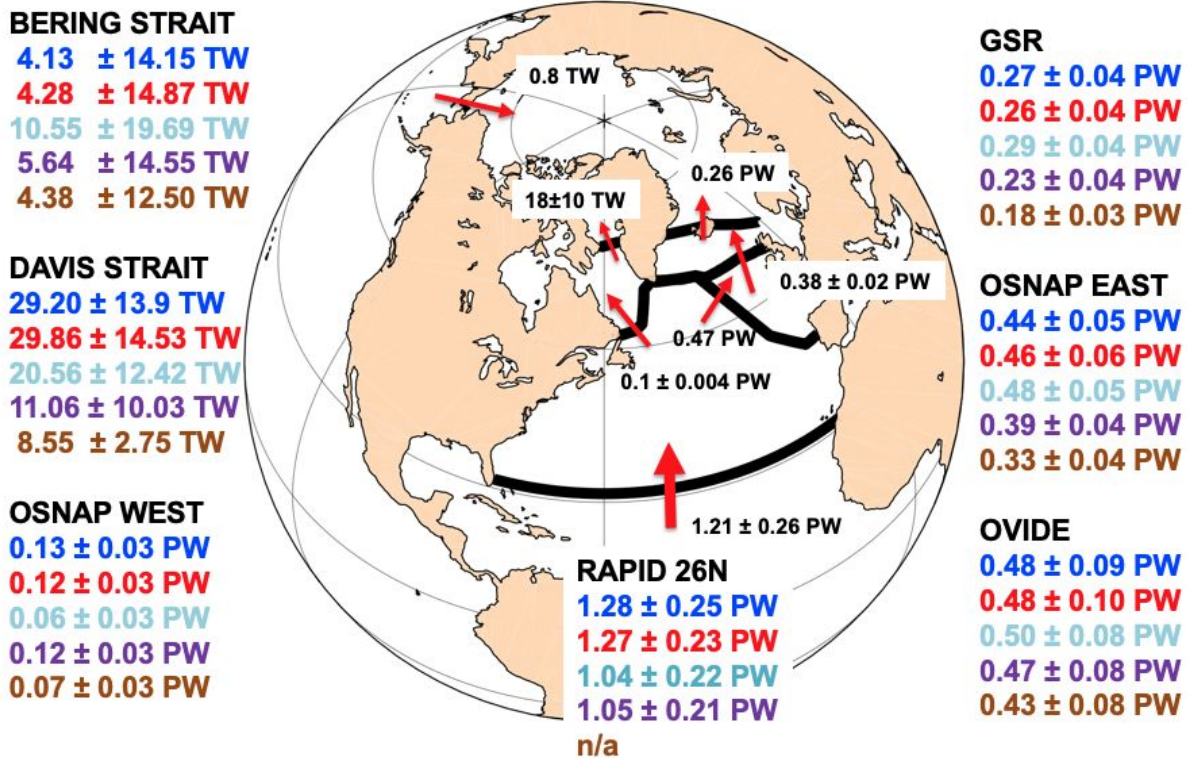


**Figure 18.** The temperature (Bering Strait, Davis Strait and GSR) and heat transports ( OSNAP East and West, OVIDE and RAPID 26°N) for each of the high resolution models. Observations are shown in black. HADGEM3 coupled CONTROL (Blue), HADGEM3 coupled HIST (red), CESMH (cyan), NEMO12 (purple) and NEMO24 (brown).

Observations of the freshwater transport in this region are limited. The transport into the Arctic through the Bering Straits and those at RAPID 26°N are known. There are measurements of the freshwater transport divergence from observation at the OSNAP Section and will be discussed in the next section. The freshwater transport from the Arctic region into the North Atlantic are generally too strong (Figure 19). The NEMO24 hindcast model has probably the best representation of the freshwater transports, but the 1/24 degree grid does not extend to the RAPID 26°N section.

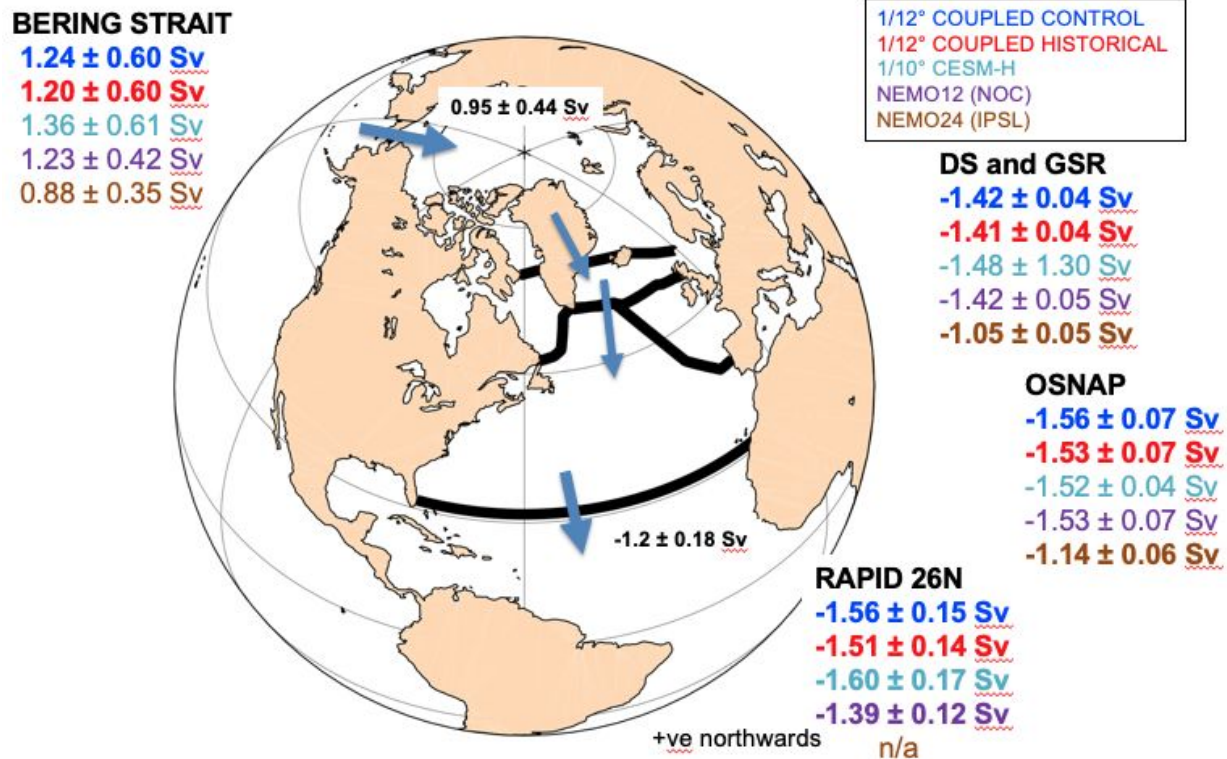


**Figure 19.** The observed and model estimates of the freshwater transports across the combined Davis Strait and Greenland Scotland Ridge, OSNAP section and RAPID 26°N.

All models do well in estimating the freshwater transport divergence. Figure 20 shows the freshwater divergence between the Bering Straits and the combined Davis Strait/Greenland Scotland Ridge, OSNAP and RAPID 26°N sections. The CESMH is slightly low in comparison to observation at all sections. The HADGEM3 Control and Historical model transports are very close across the OSNAP section (order 0.3 Sv, vs 0.33 Sv observed). They tend to underestimate the divergence at the RAPID 26°N section. The freshwater divergence between the OSNAP section and RAPID 26°N is shown in the lower box. Observation suggests that there is freshwater input/storage between OSNAP and RAPID 26°N. The models also suggest that there is storage as well (-ve term), but the HIST run is of opposite sign which may be due to the AMOC decline shown in that model. Using this method there is no way to determine where the deficiency in the system may lie, e.g. the roles of the freshwater storage, precipitation, river runoff and evaporation cannot be separated out of the calculation.

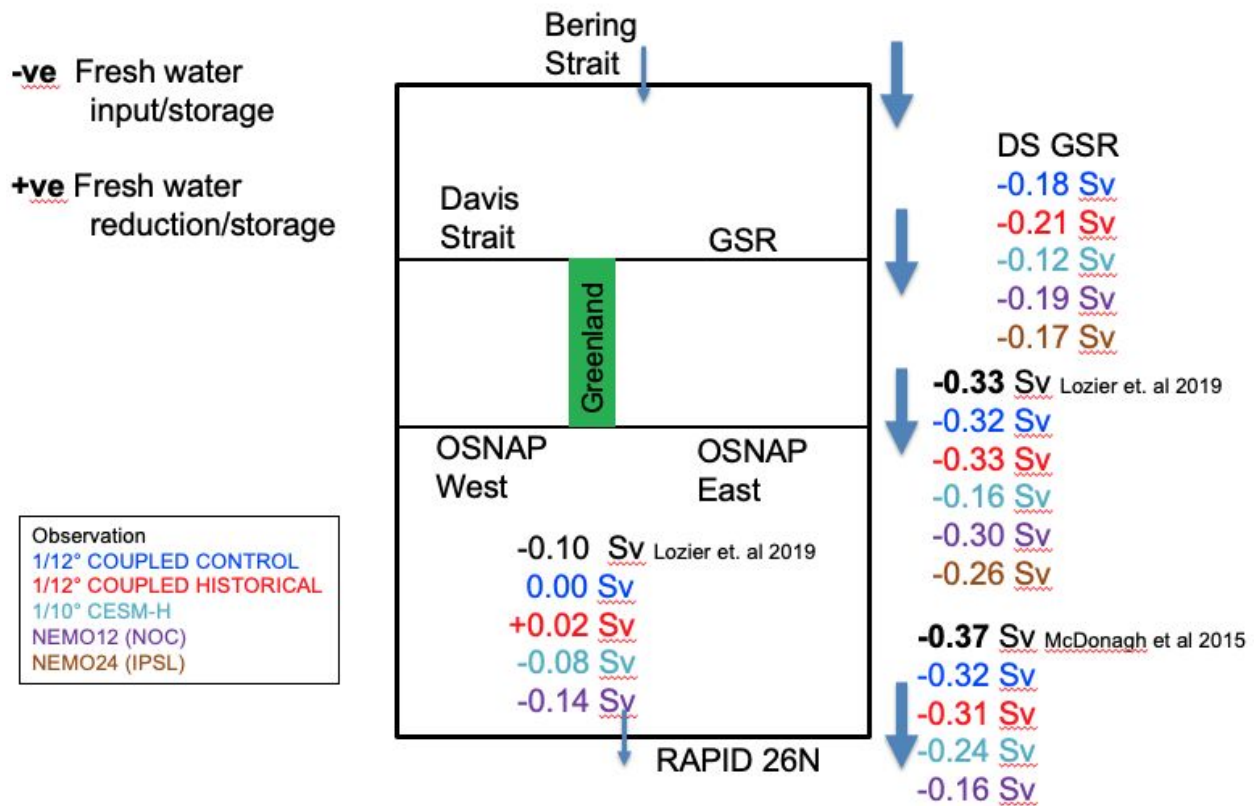


**Figure 20.** A box diagram showing the observed (black) and model estimates of the freshwater transport divergence across the combined Davis Strait and Greenland Scotland Ridge, OSNAP section and RAPID 26°N sections. The arrows show the mean direction of the freshwater transport. The values in the Box between OSNAP and RAPID show the divergence between these two sections.

### North Atlantic Heat transports in CMIP5 coupled climate models

The oceanic heat and freshwater transports in 29 Coupled Model Intercomparison Project 5th Iteration (CMIP5) models have also been calculated. Heat transport was decomposed into total heat transport, temperature-driven, velocity-driven, and residual change. Temperature and non-linear changes for each model between the approximate end of the historical (1960-1989) and approximate end of the RCP8.5 scenarios (2070-2099) was examined at 3 latitudes, 48°N, 26°N and 34°S. The next stage in the project is to examine these models to look at the response of the atmosphere to changes in the ocean heat and freshwater transport.

### Gliders: an ideal platform for sustained boundary current observations

The recent results from UK-OSNAP glider missions showed that underwater gliders can be used routinely as a component of trans-oceanic AMOC observing system to monitor the North Atlantic Current [Houpert et al., 2018; Lozier et al., 2017]. Particularly gliders appear well suited to complement an observation gap unfulfilled by TMA or satellite altimetry.

## Blue-Action Deliverable D2.1

The strengths and weaknesses of gliders [McCarthy G., et al., 2019] make them particularly relevant for boundary current monitoring: boundary currents are located close to the continental slope and their typical scales are of the order of 50 km. In addition, glider can also be operated to continuously monitor a specific location, providing data that resembles a virtual mooring/profiler. In the context of a basin-wide mooring array transmitting real-time data, this configuration could be considered as an emergency solution in case of a lost/failure of a key-mooring for the basin-wide AMOC transport calculation.

### **Relationship between AMOC, and SST and Ocean Heat content in the sub polar North Atlantic. (Moat et al. 2019)**

Moat et al. (2019) used an ocean mixed layer heat budget methodology to investigate the physical processes determining subpolar North Atlantic (SPNA) sea surface temperature (SST) and ocean heat content (OHC) variability on decadal to multidecadal time scales using the state-of-the-art climate model HadGEM3-GC2. New elements include development of an equation for the evolution of anomalous SST for interannual and longer time scales in a form analogous to that for OHC, parameterization of the diffusive heat flux at the base of the mixed layer, and analysis of a composite Atlantic meridional overturning circulation (AMOC) event. Contributions to OHC and SST variability from two sources are evaluated: 1) net ocean-atmosphere heat flux and 2) all other processes, including advection, diffusion, and entrainment for SST.

The model AMOC anomaly at 26°N is composited into different phases (Figure 22) and the respective fields of mean OHC and SST tendency were calculated. The Nordic Seas as a whole vary coherently, with OHC increasing in phases 1 and 4, and decreasing in phases 2 and 3. Of particular note is the fact that in the SPNA, in phase 4, when the AMOC is reducing, the OHC shows a warming tendency. Of particular note is the fact that in the sub polar North Atlantic, in phase 4, when the AMOC is reducing, the OHC shows a warming tendency. In the SPNA, the SST phases at 26°N bear some similarity to the observation based normalised SST trends presented in Figure 2 of Caesar et al. (2018).

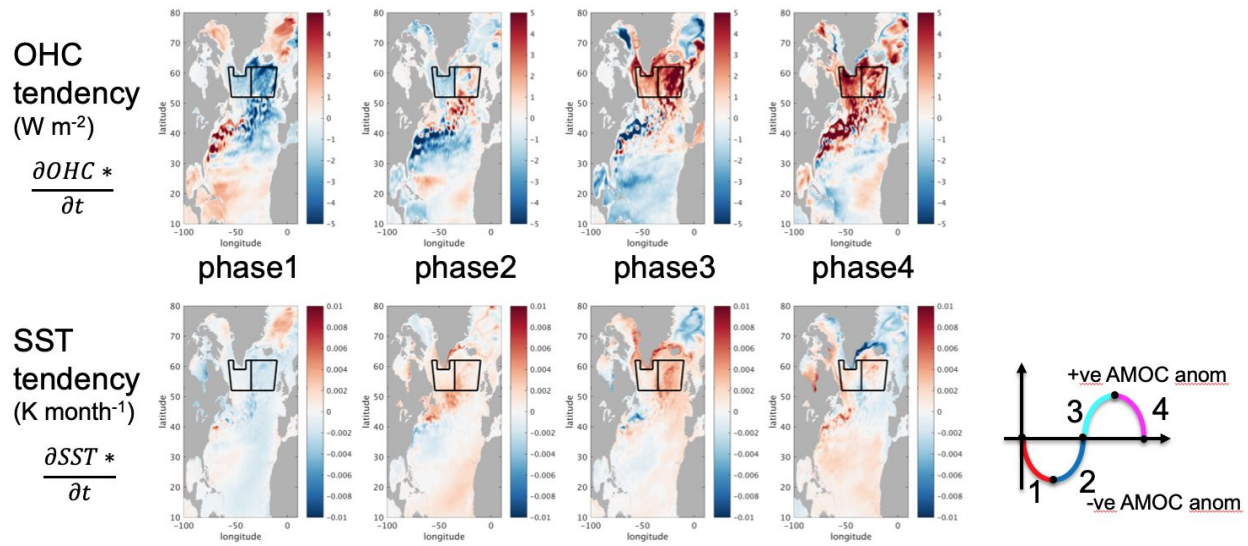


**Figure 22.** The ocean heat content and sea surface temperature tendency for each phase of the AMOC at 26°N. Reproduced from (Moat et al. 2019).

Anomalies in OHC tendency propagate anticlockwise around the SPNA on multidecadal time scales with a clear relationship to the phase of the AMOC. AMOC anomalies lead SST tendencies, which in turn lead OHC tendencies in both the eastern and western SPNA. OHC and SST variations in the SPNA on decadal time scales are dominated by AMOC variability because it controls variability of advection, which is shown to be the dominant term in the OHC budget. Lags between OHC and SST are traced to differences between the advection term for OHC and the advection–entrainment term for SST. In the western sub polar North Atlantic in particular it seems that surface fluxes drive evolution of the AMOC. This study has led to a better understanding of the relationship between AMOC and ocean heat content in the North Atlantic, which has consequences for the amount of heat leaving the Atlantic Ocean and entering the Arctic Ocean.

### Ocean precursors to the extreme Atlantic 2017 hurricane season (Hallam et. al 2019)

The 2017 Atlantic hurricane season was very active and intense and is likely to be the costliest on record. We compare 2017 to the other recent active hurricane seasons of 2005 and 2010 and identify a different driving mechanism. Precursor positive sea surface temperature anomalies (SSTA) in the main development region (MDR, 10–20°N, 20–80°W, Figure 23) favour an active hurricane season in all three years but the causes of these anomalies differ. In both 2005 and 2010, a weakening of the Atlantic Meridional Overturning Circulation (AMOC) in February and March is the primary driver of the precursor SSTA.

In contrast, in 2017, a negative wind stress curl anomaly (reducing cold water upwelling) and a positive surface net heat flux anomaly (warming the ocean) that both developed in the north eastern part of the MDR in April were the main drivers. Additionally, positive surface heat flux anomalies from May to August 2017 at the southern boundary of the MDR acted to strengthen the SSTA. The role of the

## Blue-Action Deliverable D2.1

vertical wind shear is also explored and we find that in all 3 seasons a reduction in shear occurs in concert with the positive SSTA to favour hurricane development.

The results are the first to show the importance of the AMOC in the active seasons of 2005 and 2010 and that the combination of air-sea heat flux and wind stress related processes can be an important factor in generating precursor positive SSTAs and that these processes were active pre-determinants of the 2017 hurricane season severity. Furthermore, in contrast to other recent strong seasons, in which the SSTAs were evident in March, the anomalously warm ocean surface in 2017 developed between April and July, compounding the challenge of predicting Atlantic hurricane season severity.

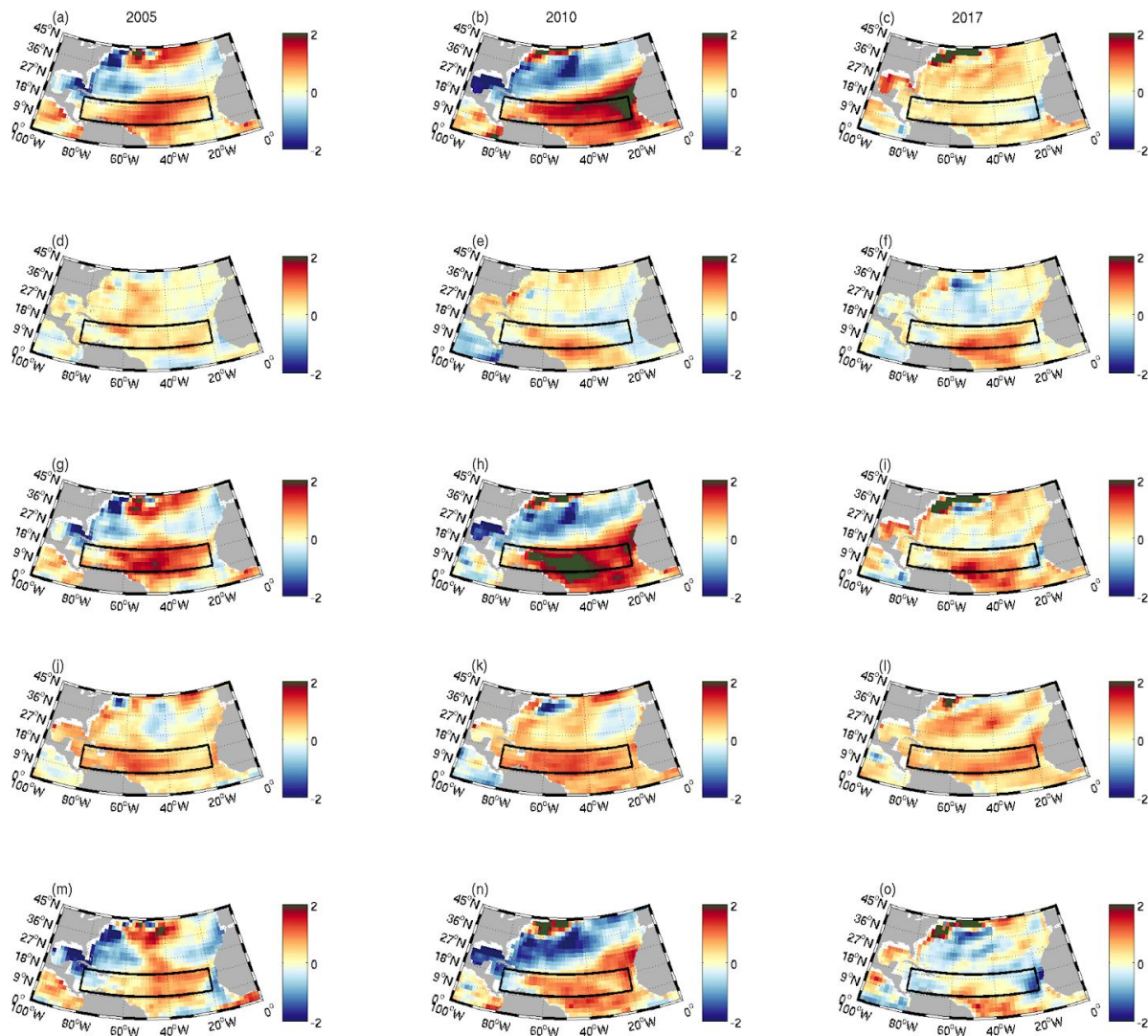


**Figure 23:** Surface Flux generated Temperature Anomaly April – July for 2005, 2010 and 2017. Initial condition – SSTA March (a - c). Estimated temperature anomaly April – July based on anomalous surface

fluxes (d - f). Estimated SSTA in August formed by summing the initial condition and April – July surface flux generated temperature anomaly (g - i). Observed SSTA in August (j - l). Estimated minus observed August SSTA (m - o). Black box indicates MDR region. (from Hallam et al. 2019)

## Progress beyond the state of the art

- The CMIP6 models are commonly referred to as state-of-the-art. The very high resolution coupled models used in this study were run by the UK funded **ACSIS programme and the H2020 programme PRIMAVERA. They are of a higher ocean and atmospheric resolution than CMIP6, and are truly beyond the state of the art.** The evaluation performed in this study gives these 'above' the state-of-the-art models a baseline for further studies in the years to come.
- The **Glider surveys** undertaken as part of OSNAP are groundbreaking in terms of the findings and the length of time they were used and their contribution the mooring array.
- For the first time we have a better understanding of the link between **variability in the AMOC on decadal time scales and its effect on ocean heat content and sea surface temperature** (Moat et al. 2019). This will lead to **better decadal prediction of European climate.**

## Impact

### How has this work contributed to the expected impacts of Blue-Action?

#### **Improve capacity to predict the weather and climate of the Northern Hemisphere, and make it possible to better forecast of extreme weather phenomena**

Through optimized use of data, closing data gaps, increased operability and utility, improved representation of Arctic-lower latitude linkages.

#### **Improve the uptake of measurements from satellites by making use of new Earth observation assets**

Earth observations from space of the cryosphere and ocean surface state in particular are essential assets for assessing model performance and the basis for developing improved process representation. Blue-Action improves the uptake by combining in-situ measurements from ocean mooring systems, new ocean observing platforms and data from existing and upcoming satellite missions to produce a valid view of ocean heat anomaly propagation towards the Arctic.

#### **Lead to optimised observation systems for various modelling applications**

Targeted systems for optimisation include the comprehensive moored observatories designed to monitor ocean exchanges and operated semi-operationally in the Atlantic and at the gateways to the Arctic. Optimization facilitates enhanced exploitation and is focussed on operability, fast data return and closing data gaps. Coordination of efforts and the added value of estimates (near-real-time and delayed) will further enhance their utility for validation of model systems.

#### **Improving the professional skills and competences for those working and being trained to work within**

### **this subject area and improving innovation capacity and the integration of new knowledge**

Through collaborative policy briefings addressing policy makers involved in determining key policy issues relating to weather and oceanic observation systems.

## **Lessons learned and Links built**

- D2.1 has provided decadal transports and their variability to deliverable D2.2 Observed ocean, processes, mechanisms of subpolar gyre circulation and propagation of heat anomalies.
- D2.1 has provided high resolution model transports to D2.3 Processes and flow over the iceland-Faroe Ridge and D2.4 Synthesis and dissemination of ocean and atmosphere heat transport to the Arctic. With co-authored a paper with D2.4
- D2.1 has contributed to the Cost-benefit analysis of the RAPID and OSNAP arrays in D2.7.
- We Interacted with the PRIMAVERA group via Skype 22nd May 2019 to present the latest evaluation results of their very high resolution model. Throughout the Blue-Action project we maintained communication with PRIMAVERA by links built with Malcolm Roberts at the UK Met office.
- Ben Moat contributed to **Workshop on ESM evaluation: *Evaluating climate and Earth system models at the process level***, 23-24 May 2017. This was a joint workshop between four H2020 projects (**CRESCENDO, PRIMAVERA, Blue-Action and APPLICATE**) plus members of other FP7 invited projects (**BACCHUS, STRATOCLIM, DACCIWA, IS-ENES2, ICE-ARC, IMPREX**). This lead to the promotion of Blue-Action activities and gave the modelling community an overview of the metrics from ocean observations that are available for model evaluation. It brought Blue-Action and PRIMAVERA together to discuss the results of the very high resolution analysis. (Ben Moat's talk available at : <https://zenodo.org/record/1248523>)
- Partners from WP2 contributed to a SEARICA Science-policy breakfast discussion with MEP's: "The slowing Gulf Stream? What we know and potential impacts" at the European Parliament, Brussels (BE) on the 4th September 2018. The policy brief is available via <https://zenodo.org/record/1408097> The related deliverable is the D8.11.

## **Contribution to the top level objectives of Blue-Action**

### **Objective 1 Improving long range forecast skill for hazardous weather and climate events**

Sinha et al. (2019) has shown that there is a quick response feedback mechanism which connects the Arctic ocean to the North Atlantic. Changes in the Arctic are transferred quickly via internal waves to the North Atlantic which leads to changes in the AMOC strength and variability.

### **Objective 2 Enhancing the predictive capacity beyond seasons in the Arctic and the Northern Hemisphere**

Moat et al. (2019) has shown that there are predictable decadal cycles in the sea surface temperature and ocean heat content of the North Atlantic which vary with the AMOC. Linking this predictability will

## **Blue-Action Deliverable D2.1**

improve our understanding of the Atlantic Multidecadal Variability and the associated cycles in European climate.

### **Objective 3 Quantifying the impact of recent rapid changes in the Arctic on Northern Hemisphere climate and weather extremes**

Sinha et al. (2019) has shown that there is a quick response feedback mechanism which connects the Arctic ocean to the North Atlantic. Changes in the Arctic are transferred quickly via internal waves to the North Atlantic which leads to changes in the AMOC strength and variability.

### **Objective 4 Improving the description of key processes controlling the impact of the polar amplification of global warming in prediction systems**

We have determined the heat transport into the Arctic from the very high resolution climate models. The transport of heat into the Arctic is one process contributing to Arctic Amplification.

### **Objective 5 Optimizing observational systems for predictions**

Currently there are observations of the AMOC and associated heat and freshwater transports at 26°N in the North Atlantic from 2004 to present. In this deliverable we have undertaken a study to extend the RAPID 26°N AMOC time series to the whole satellite era and develop a framework to deliver the AMOC in near real time.

### **Objective 6 Reducing and evaluating the uncertainty in prediction systems**

Prediction systems depend on the quality of the models underlying them. Models need to be validated against observations to understand how well they simulate the real world. This deliverable has provided beyond state-of-the-art assessment of this ability to simulate the real world thus improving understanding of the capabilities of prediction systems.

### **Objective 7 Fostering the capacity of key stakeholders to adapt and respond to climate change and boosting their economic growth**

The Moat et al. (2019) paper has lead to a better understanding/potential prediction of Atlantic/Arctic decadal variability. This will lead to improved planning to adapt to changes in european climate in future years.

### **Objective 8 Transferring knowledge to a wide range of interested key stakeholders**

- Partners from WP2 contributed to a SEARICA Science-policy breakfast discussion with MEP's: "The slowing Gulf Stream? What we know and potential impacts".
- Work package leader Karin Margretha Larsen and D2.1 lead Ben Moat were invited to attend the 'Impact assessment study on societal benefits of Arctic observing systems' (IMOBAR) workshop on the 23-24 Nov 2017 in Brussels (BE). The aim of the workshop is to bring together experts in observations, observational data providers, major users and stakeholders in order to discuss the

societal benefit areas of Arctic observational systems. The workshop provided information on relative importance of observational systems with respect to their societal benefits and investment and maintenance costs. A report is available via: <https://publications.jrc.ec.europa.eu/repository/bitstream/JRC113327/kjna29400enn.pdf>

## References (Bibliography)

- Berx, B., Hansen, B., Østerhus, S., Larsen, K. M. H., Sherwin, T., Jochumsen, K. 2013. Combining in situ measurements and altimetry to estimate volume, heat and salt transport variability through the Faroe–Shetland Channel, *Ocean Sci.*, 9, 639–654, <https://doi.org/10.5194/os-9-639-2013>.
- Caesar L., S. Rahmstorf, A. Robinson, G. Feulner & V. Saba, 2018, Observed fingerprint of a weakening Atlantic Ocean overturning circulation, *Nature*, 556, 191–196
- Curry, B., C.M. Lee, B. Petrie, R.E. Moritz, and R. Kwok, 2014: Multiyear Volume, Liquid Freshwater, and Sea Ice Transports through Davis Strait, 2004–10. *J. Phys. Oceanogr.*, **44**, 1244–1266, <https://doi.org/10.1175/JPO-D-13-0177.1>
- Desbruyeres, Damien; McDonagh, Elaine L.; King, Brian A.; Thierry, Virginie. 2017 Global and full-depth ocean temperature trends during the early 21st century from Argo and repeat hydrography. *Journal of Climate*, 30 (6). 1985-1997. <https://doi.org/10.1175/JCLI-D-16-0396.1>
- Desbruyeres, D.G.; McDonagh, E.L.; King, B.A.; Garry, F.K.; Blaker, A.T.; Moat, B.; Mercier, H.. 2014 Full-depth temperature trends in the Northeastern Atlantic through the early 21st century. *Geophysical Research Letters*, 41 (22). 7971-7979. <https://doi.org/10.1002/2014GL061844>
- Frajka-Williams (2015). Estimating the Atlantic overturning at 26°N from altimetry and cable measurements, *Geophysical Research Letters*, 42.3458-3464. <https://doi.org/10.1002/2015GL063220>
- Hansen, B., Larsen, K. M. H., Hátún, H., Kristiansen, R., Mortensen, E., Østerhus, S. 2015. Transport of volume, heat, and salt towards the Arctic in the Faroe Current 1993–2013, *Ocean Sci.*, 11, 743–757, <https://doi.org/10.5194/os-11-743-2015>.
- Gaillard, F., T. Reynaud, V. Thierry, N. Kolodziejczyk, and K. von Schuckmann, 2016: In Situ–Based Reanalysis of the Global Ocean Temperature and Salinity with ISAS : Variability of the Heat Content and Steric Height. *J. Clim.*, **29**, 1305–1323, doi:10.1175/JCLI-D-15-0028.1.
- Hansen, B., Larsen, K. M. H., Hátún, H. 2019a. Monitoring the velocity structure of the Faroe Current. Havstovan Technical Report 19-01, <http://www.hav.fo/PDF/Ritgerdir/2019/TechRep1901.pdf>.
- Hansen, B., Larsen, K. M. H., Hátún, H., Jochumsen, K., Østerhus, S. 2019b. Monitoring the hydrographic structure of the Faroe Current. Havstovan Technical Report 19-02, <http://www.hav.fo/PDF/Ritgerdir/2019/TechRep1902.pdf>.
- Johns W.E., Baringer M.O, Beal L.M., Cunningham S.A., Kanzow T., Bryden H.L., Hirschi J.J.-M., Marotzke J., Meinen C.S., Shaw B. and Curry R., 2011, Continuous, array-based estimates of Atlantic Ocean heat transport at 26.5°N, *Journal of Climate*. 24(10), 2429-2449.

## Blue-Action Deliverable D2.1

- Levitus, S., J. I. Antonov, T. P. Boyer, H. E. Garcia, and R. a. Locarnini, 2005: Linear trends of zonally averaged thermosteric, halosteric, and total steric sea level for individual ocean basins and the world ocean, (1955-1959)-(1994-1998). *Geophys. Res. Lett.*, **32**, 1–4, doi:10.1029/2005GL023761.
- Liblik, T., Karstensen, J., Testor, P., Alenius, P., Hayes, D., Ruiz, S., ... Mauri, E. (2016). Potential for an underwater glider component as part of the Global Ocean Observing System. *Methods in Oceanography*. <https://doi.org/10.1016/j.mio.2016.05.001>
- Madec, G. (2008), NEMO Ocean Engine, Note du Pole de Modélisation, vol. 27, 1288–1619, Inst. Pierre-Simon Laplace, Paris, France.
- McCarthy, G. D., Smeed, D. A., Johns, W. E., Frajka-Williams, E., Moat, B. I., Rayner, D., ... & Bryden, H. L. (2015). Measuring the Atlantic meridional overturning circulation at 26 N. *Progress in Oceanography*, **130**, 91-111.
- Mercier, H., and Coauthors, 2015: Variability of the meridional overturning circulation at the Greenland–Portugal OVIDE section from 1993 to 2010. *Prog. Oceanogr.*, **132**, 250–261, doi:10.1016/j.pocean.2013.11.001.<http://www.sciencedirect.com/science/article/pii/S0079661113002206>.
- Lozier, M.S., F. Li, S. Bacon, F. Bahr, A.S. Bower, S.A. Cunningham, M.F. de Jong, L. de Steur, B. deYoung, J. Fischer, S.F. Gary, B.J.W. Greenan, N.P. Holliday, A. Houk, L. Houpert, M.E. Inall, W.E. Johns, C. Johnson, J. Karstensen, G. Koman, I.A. Le Bras, X. Lin, N. Mackay, M. Oltmanns, R.S. Pickart, A.L. Ramsey, D. Rayner, F. Straneo, D.J. Torres, I. Yashayaev, J. Zhao (2019). Meridional overturning circulation and the associated heat and freshwater transports observed by the OSNAP (Overturning in the Subpolar North Atlantic Program) Array from 2014 to 2016. Duke Digital Repository. <https://doi.org/10.7924/r4z60gf0f>
- McDonagh, E.L., B.A. King, H.L. Bryden, P. Courtois, Z. Szuts, M. Baringer, S.A. Cunningham, C. Atkinson, and G. McCarthy, 2015: Continuous Estimate of Atlantic Oceanic Freshwater Flux at 26.5°N. *J. Climate*, **28**, 8888–8906, <https://doi.org/10.1175/JCLI-D-14-00519.1>
- Moat, B.I.; Josey, S.A.; Sinha, B.; Blaker, A.T.; Smeed, D.A.; McCarthy, G.; Johns, W.E.; Hirschi, J.-M.; Frajka-Williams, E.; Rayner, D.; Duchez, A.; Coward, A.C.. 2016, Major variations in subtropical North Atlantic heat transport at short (5 day) timescales and their causes. *Journal of Geophysical Research: Oceans*, **121** (5). 3237-3249.<https://doi.org/10.1002/2016JC011660>.
- Svein Østerhus, Rebecca Woodgate, Héðinn Valdimarsson, Bill Turrell, Laura de Steur, Detlef Quadfasel, Steffen M. Olsen, Martin Moritz, Craig M. Lee, Karin Margretha H. Larsen, Steingrímur Jónsson, Clare Johnson , Kerstin Jochumsen, Bogi Hansen, Beth Curry, Stuart Cunningham, and Barbara Berx , 2019, Arctic Mediterranean exchanges: a consistent volume budget and trends in transports from two decades of observations, *Ocean Sci.*, **15**, 379-399, <https://doi.org/10.5194/os-15-379-2019>
- Roberts, M. J., Baker, A., Blockley, E. W., Calvert, D., Coward, A., Hewitt, H. T., Jackson, L. C., Kuhlbrodt, T., Mathiot, P., Roberts, C. D., Schiemann, R., Seddon, J., Vannière, B., and Vidale, P. L., 2019, Description of the resolution hierarchy of the global coupled HadGEM3-GC3.1 model as used in CMIP6 HighResMIP experiments, *Geosci. Model Dev. Discuss.*, <https://doi.org/10.5194/gmd-2019-148>, in review.
- Small et al. 2014, A new synoptic scale resolving global climate simulation using the Community Earth System Model, *J. of Advances in Earth System Models*, **6**, <https://doi.org/10.1002/2014MS000363>
- Smeed D.; McCarthy G.; Rayner D.; Moat B.I.; Johns W.E.; Baringer M.O.; Meinen C.S. (2017). Atlantic meridional overturning circulation observed by the RAPID-MOCHA-WBTS (RAPID-Meridional Overturning Circulation and Heatflux Array-Western Boundary Time Series)

## Blue-Action Deliverable D2.1

array at 26°N from 2004 to 2017. British Oceanographic Data Centre - Natural Environment Research Council, UK. doi: 10.5285/5acfd143-1104-7b58-e053-6c86abc0d94b

- Testor, P., DeYoung, B., Rudnick, D. L., Glenn, S., Hayes, D., Lee, C., ... & Alenius, P. (2019). OceanGliders: a component of the integrated GOOS. *Frontiers in Marine Science*, 6, 422.
- Woodgate, R.A., 2018, Increases in the Pacific inflow to the Arctic from 1990 to 2015, and insights into seasonal trends and driving mechanisms from year-round Bering Strait mooring data, *Progress in Oceanography*, 160, 124-154, doi:10.1016/j.pcean.2017.12.007.

## Dissemination and exploitation of Blue-Action results

### Dissemination activities

| Type of dissemination activity  | Name of the scientist (institution), title of the presentation, event  | Place and date of the event       | Type of Audience   | Estimated number of persons reached | Link to Zenodo upload   |
|---|--|-----------------------------------|--|-------------------------------------|---|
| Participation in activities organised jointly with other H2020 project(s) | Ben Moat (NOC), presentation on "Evaluating North Atlantic ocean circulation and properties, Evaluating climate and Earth System models at the process level" at the EC Workshop Evaluating climate and Earth system models at the process level | Brussels (BE), 23-24 May 2017     | Scientific Community (higher education, Research), Policy makers | 30                                  | <a href="https://doi.org/10.5281/zenodo.1248523">https://doi.org/10.5281/zenodo.1248523</a>   |
| Participation to a conference   | Ben Moat (NOC), Transport of freshwater and heat in the subtropical North Atlantic, Understanding Change and Variability in the North Atlantic Climate System, ACSIS - OSNAP - RAPID Joint Science Meeting                                       | Oxford (UK), 19-21 September 2017 | Scientific Community (higher education, Research)                | 100                                 | <a href="https://doi.org/10.5281/zenodo.1248505">https://doi.org/10.5281/zenodo.1248505</a>   |
| Participation to a conference   | Ben Moat (NOC), Relationship between changes in the AMOC, North Atlantic heat content and SST., Understanding Change and Variability in the North Atlantic Climate System, ACSIS - OSNAP - RAPID Joint Science Meeting                           | Oxford (UK), 19-21 September 2017 | Scientific Community (higher education, Research)                | 100                                 | <a href="https://doi.org/10.5281/zenodo.1248497">https://doi.org/10.5281/zenodo.1248497</a>   |
| Participation in activities organised jointly with                        | Ben Moat (NOC), Karin Larsen (HAV), Impact Assessment on a Long-Term Investment on Arctic Observations, IMOBAR workshop  | Brussels (BE), 23-24 November     | Policy makers, Scientific Community (higher                      | 50                                  | <a href="https://publications.jrc.ec.europa.eu/repository/bitstream/">https://publications.jrc.ec.europa.eu/repository/bitstream/</a> |

**Blue-Action Deliverable D2.1**

|   |  |                                    |   |     |   |
|---|--|------------------------------------|---|-----|---|
| other H2020 project(s)  |  | 2017                               | education, Research)  |     | <a href="https://doi.org/10.5281/zenodo.1248531">JRC113327/kjna29400enn.pdf</a>             |
| Participation to a conference   | Ben Moat (NOC), High resolution model-observation comparison at key locations for heat and freshwater transport to the Arctic, Blue-Action 2018 Annual Meeting   | Bologna (IT), 18-19 January 2018   | Scientific Community (higher education, Research), Civil Society, Industry, Policy makers | 20  | <a href="https://doi.org/10.5281/zenodo.1248531">https://doi.org/10.5281/zenodo.1248531</a> |
| Participation to a conference   | Ben Moat (NOC), Relationship between changes in the AMOC, North Atlantic heat content and SST, AGU Ocean Sciences Meeting  | Portland (US), 11-16 February 2018 | Scientific Community (higher education, Research)   | 500 | <a href="https://doi.org/10.5281/zenodo.1248474">https://doi.org/10.5281/zenodo.1248474</a> |
| Participation to a conference   | Ben Moat (NOC), Relationship between changes in the AMOC and North Atlantic sea surface temperature, ACSIS Ocean-Ice Theme Science Day NOC   | Southampton (UK), 27 April 2018    | Scientific Community (higher education, Research)   | 20  | <a href="https://doi.org/10.5281/zenodo.1248516">https://doi.org/10.5281/zenodo.1248516</a> |
| Participation in activities organised jointly with other H2020 project(s) | Policy Briefing “The slowing Gulf Stream? What we know and potential impacts” with Presentations were given from: Steffen Olsen (DMI), Tor ELDEVIK (UIB), Ben Moat (NOC), Karin Margretha Larsen (HAV), Marilena Oltmanns (GEOMAR), Marius Årthun (UIB), held at the European Parliament | Brussels (BE), 4 September 2018    | Policy makers   | 50  | <a href="http://doi.org/10.5281/zenodo.1408097">http://doi.org/10.5281/zenodo.1408097</a>   |
| Participation to a conference   | Ben Moat (NOC), New insights into decadal North Atlantic SST and OHC variability from a coupled climate model, at EGU 2019   | Vienna (At), 7-12 April 2019       | Scientific Community (higher education, Research)   | 100 | <a href="https://zenodo.org/record/3475949">https://zenodo.org/record/3475949</a>           |
| Participation to a conference   | Ben Moat (NOC), New insights into decadal North Atlantic SST and OHC variability from a coupled climate model, at IUGG   | Montreal (CAN), 8-18 July 2019     | Scientific Community (higher education, Research)   | 100 | <a href="https://zenodo.org/record/3475968">https://zenodo.org/record/3475968</a>           |
| Participation to a conference   | Ben Moat (NOC), New insights into decadal North Atlantic SST and OHC variability from a coupled climate model, at ACSIS project meeting, British Antarctic Survey  | Cambridge (UK), 17-18 July 2019    | Scientific Community (higher education, Research)   | 100 | <a href="https://zenodo.org/record/3475992">https://zenodo.org/record/3475992</a>           |

## Blue-Action Deliverable D2.1

|                               |   |                                    |   |    |   |
|-------------------------------|---|------------------------------------|---|----|---|
| Participation to a conference | Ben Moat (NOC), Insights into decadal North Atlantic sea surface temperature and ocean heat content variability from an eddy-permitting coupled climate model, Blue-Action General Assembly | Edinburgh (UK), 15-17 October 2019 | Scientific Community (higher education, Research), Civil Society, Industry, Policy makers | 50 | <a href="https://www.zenodo.org/communities/blue-actionh2020/">https://www.zenodo.org/communities/blue-actionh2020/</a> |
|-------------------------------|---|------------------------------------|---|----|---|

## Peer reviewed articles

| Title   | Authors  | Publication                                   | DOI   | Is Blue-Action correctly acknowledged? | Open Access granted |
|---|--|---|---|--|---------------------|
| Insights into decadal North Atlantic sea surface temperature and ocean heat content variability from an eddy-permitting coupled climate model | B. I. Moat, B. Sinha, S. A. Josey, J. Robson, P. Ortega, F. Sevellec, N. P. Holliday, G. D. McCarthy, A. L. New, J. J.-M. Hirschi, | Journal of climate                            | 10.1175/JCLI-D-18-0709.1  | YES                                    | Yes                 |
| Structure and transport of the North Atlantic current in the Eastern Subpolar Gyre from sustained glider observations.                        | Houpert, L., Inall, M. E., Dumont, E., Gary, S., Johnson, C., Porter, M., Johns, W. E., Cunningham, S,                             | Journal of Geophysical Research: Oceans, 123, | 10.1029/2018JC014162  | yes                                    | yes                 |
| Ocean precursors to the extreme Atlantic 2017 hurricane season  | Samantha Hallam, Robert Marsh, Simon A. Josey, Pat Hyder, Ben Moat & Joël J.-M. Hirschi  | Nature Communications 10, 679                 | <a href="https://doi.org/10.1038/s41467-019-08496-4">https://doi.org/10.1038/s41467-019-08496-4</a> | yes                                    | yes                 |
| Atlantic Meridional Overturning Circulation: Observed Transport and Variability   | Frajka-Williams et al. 2019  | Front. Mar. Sci                               | <a href="https://doi.org/10.3389/fmars.2019.00260">https://doi.org/10.3389/fmars.2019.00260</a>     | yes                                    | yes                 |

## Other publications

These are the publications currently in preparation, submitted, in review, accepted:

## Blue-Action Deliverable D2.1

- McCarthy et al. 2019, Sustainable observations of the AMOC: Methodology and Technology, Reviews of Geophysics, accepted.
- Hirschi, J. t al. 2019, The Atlantic meridional overturning circulation in high resolution models, Journal of Geophysical Research - Oceans, in review
- Sinha, B, B. Topliss, M. Hughes, A. T. Blaker, J. Hirschi, C. Franzke, S. A. Josey, V. Ivchenko, B. I. Moat, Impact of Arctic climate change on the North Atlantic ocean circulation: a model study, Journal of Geophysical Research - Oceans, submitted
- Harry Bryden; William E. Johns; Brian A. King; Gerard McCarthy; Elaine L. McDonagh; Ben I. Moat; David A. Smeed, Reduction in ocean heat transport at 26°N since 2008 cools the eastern subpolar gyre of the North Atlantic Ocean, Journal of climate, accepted
- A. Sanchez-Franks, E. Frajka-Williams, B. Moat, Full depth Transport Estimates of the Atlantic Overturning at 26°N from Altimetry and GRACE, Geophysical Research Letters, in prep.

### Uptake by the targeted audiences

As indicated in the Description of the Action, the audience for this deliverable is the general public (PU) is and is made available to the world via CORDIS.

### This is how we are going to ensure the uptake of the deliverables by the targeted audiences:

- Through dissemination at relevant scientific events (EGU...).
- Through dissemination to relevant non scientific audiences, such as civil society, businesses and policy makers: see D8.8 Societal Engagement Knowledge Exchange Nr. 2, on Ocean observations and predictions in response to the climate emergency.